Influence of Displacement Rate on the Direct Shear Strength Characteristics of Reconstituted Varved Couplets Prepared with Various Moisture Content

Deepali Anand[1], Arindam Dey[1] and Ravi K.[1*]

Deepali Anand

Research Scholar, Department of Civil Engineering, Indian Institute of Technology Guwahati, Assam, India. ORCID No.: 0000-0002-0072-2236 Email: a.deepali@iitg.ac.in

Arindam Dey*

Associate Professor, Department of Civil Engineering, Indian Institute of Technology Guwahati, Assam, India. ORCID No.:0000-0001-7007-2729 Contact No.: +918011002709 Email: arindamdeyiitg16@gmail.com

* Corresponding author

Ravi K.

Associate Professor, Department of Civil Engineering, Indian Institute of Technology Guwahati, Assam, India. ORCID No.: 0000-0002-3152-1533 Email: ravi.civil@iitg.ac.in

Funding and Acknowledgment: This study belongs to a part of the project 'Study of Glacial Dynamics and Sustainable Hydrological Resources in Arunachal Himalaya' (Project No. DST/CCP/MRDP/ 185/2019(G) dated 13/03/2020). The project is supported by Department of Science & Technology (SPLICE – Climate Change Program), Ministry of Science and Technology, Govt. of India. The authors express their gratitude for receiving the financial support for the same.

Compliance with Ethical Standards

Conflict of Interest: The authors declare that they have no known competing financial interests or personal relationships that could have appeared to influence the work reported in this paper.

Ethical Approval: This article does not contain any studies with human participants or animals performed by any of the authors.

Author Contributions: DA: Conceptualization, Formal analysis, Investigation, Writing – Original preparation; AD: Funding Acquisition, Supervision, Revision and Editing of drafted manuscript; RK: Funding acquisition, Supervision

Data Availability Statement: The data pertaining to and reported in this study is available from the corresponding author upon reasonable request.

Influence of Displacement Rate on the Direct Shear Strength Characteristics of Reconstituted Varved Couplets Prepared with Various Moisture Content

Abstract

This study investigates the shear strength behavior of homogeneous and reconstituted varved clay couplets samples under varying normal stresses (50, 100, and 150 kPa), shearing displacement rates (1.25, 0.24, and 0.024 mm/min), and moisture conditions (dry, 0.8 OMC, OMC, 1.2 OMC, and submerged) through a series of Direct Shear Tests (DST). It is hypothesized that different applied normal stresses on the samples simulate varying stress conditions caused by glacier accumulation, and the displacement rates replicate the velocity of glacial movement over soil. The results reveal that shear strength parameters—cohesion and internal friction angle—and the peak shear stresses at failure under different normal stresses are significantly affected by moisture conditions and displacement rates. The increase in normal stresses leads to higher peak shear stresses at failure. A decrease in displacement rate at which the sample is sheared results in an increase in shear strength parameters and shear stresses. As the moisture content increases, angle of internal friction and cohesion of the samples initially rise, reaching peak magnitudes between the moisture contents of 0.8 OMC and OMC. Both parameters then decrease with further increases in moisture until submerged conditions are reached. For all displacement rates, the maximum angle of internal friction and cohesion in the reconstituted varve couplet is achieved at both drier and wetter moisture conditions, relative to the peak values of internal friction and cohesion in homogeneous soil samples. Therefore, it is necessary to consider the interface characteristics in laminated soil structures when characterizing them for engineering purposes.

Keywords: Reconstituted varved clay couplet, Direct shear test, Displacement rate, Moisture conditions variation, Shear strength

1. Introduction

Due to a variety of sedimentation processes, soil deposits formed in glacial regions are among the most complex in all geologic environments (Chung and Finno, 1992; Mark and Fernández, 2022). This complexity arises because the formation of glacial soils is influenced by factors such as meltwater supply from glaciers, and crustal loading and unloading from glaciers or ice sheets (Eyles and Lazorek, 2013). Deposits formed in such environments often consist of poorly sorted particles and may be stratified (Eyles and Lazorek, 2013; Menzies and van der Meer, 2018). Even after soil deposition in glacial settings, deposits may be further sheared due to glacial activities such as accumulation, ablation, and glacier movement, which impacts its shear failure envelope (Altuhafi *et al.*, 2009; Altuhafi *et al.*, 2010). Studies by Boulton and Dobbie (1998), Boulton *et al.* (2001), and Huo *et al.* (2021) have examined shear deformation in soil beds due to glacier movement. However, these studies generally focus on geomorphological features formed by shearing during glacial override over soils. The increase in geo-disasters in cold regions over recent decades has drawn attention of researchers to the geotechnical aspects of glacial loading and override, though such studies are still in their infancy. Additionally, increasing construction in permafrost regions has made it crucial to understand factors affecting soil strength properties in cold regions (Du *et al.*, 2016). Glacial override, the process by which glaciers move over existing soils, influences the strength, deformation, and stability of soils, especially given the presence of moisture. Variation in water content and its impact on soil shear strength has long been of interest to geotechnical engineers and is recognized as a significant factor affecting shear strength (Horn and Albrechts, 2002; Abdullahi *et al.*, 2022). Slope failure during loading is also influenced by moisture levels in the soil (Zhou *et al.*, 2019). Soils containing clay minerals are particularly sensitive to changes in moisture conditions (Bláhová *et al.*, 2013). This study addresses these gaps by conducting direct shear tests (DST) on three different soil samples under various combinations of applied normal stresses, displacement rates, and moisture conditions. The variables considered in DST simulate different conditions of the glacial environment. The varying applied normal stresses simulate glacial load, while the displacement rate at which the soil sample is sheared represents the velocity of glacial override. The combined action of glacial load and movement results in the remolding of underlying soils prepared under different moisture conditions.

There are very few studies that have explored the variation in shear strength behavior of soils with changes in normal stresses, displacement rate, and moisture content. Cokca *et al.* (2004) investigated the impact of different moisture conditions and soaking on the shear strength

parameters of clay through DST. The water content in the soil was chosen with reference to Optimum Moisture Content (OMC), with three moisture contents on the dry side of OMC and three on the wet side of OMC, including a soaked sample. A decrease in the friction angle with increasing moisture content was reported. The magnitude of cohesion rapidly increased for moisture content on the dry side of OMC, but near OMC and on its wetter side, a drop in cohesion magnitude was observed. Additionally, soaking of the sample did not affect the friction angle of the soil; however, it reduced cohesion by threefold. Thermann *et al.* (2006) studied shear strength by conducting DST on heterogeneous till by varying several factors, including displacement rate. Out of the three displacement rates of 0.5, 0.05, and 0.005 mm/min at which the experiment was carried out, the lowest shear stress was obtained for samples sheared at a displacement rate of 0.05 mm/min. Mamo *et al.* (2015) examined the effect of varying displacement rates on the internal friction angle of sand samples prepared at different relative densities. The internal friction angle was found to increase with relative density. Among the three chosen displacement rates of 0.035, 0.0069, and 0.0014%/s, the internal friction angle was highest for the intermediate displacement rate of 0.0069%/s. Additionally, the variation in friction angle with the applied displacement rate was more pronounced as the relative density of the soil increased. Zhou *et al.* (2019) studied the variation in shear behavior of glacial tills, compacted at different moisture contents ranging from 10% to 18% and under various normal stresses. An increase in shear strength and shear strength parameters was observed as normal stresses increased, while a decreased dilation rate was observed as water content increased at all applied normal stresses. It was also found that while apparent cohesion decreased with increasing moisture content, the internal friction angle remained unchanged. Flieger-Szymanska *et al.* (2019) conducted DST on varved clays by separately testing its dark-colored and light-colored lamina. The friction angle was lower, and cohesion was higher in the dark-colored lamina compared to the light-colored lamina. Beren *et al.* (2020) conducted DST on sand samples at various displacement rates ranging from 0.05 to 5 mm/min. It was reported that the friction angle increased with increasing displacement rate, while cohesion decreased. However, shear stress increased with increasing displacement rate at various applied normal stresses. Basudhar *et al.* (2020) conducted DST on two types of sands, one with smooth grains and the other with angular grains. It was found that the internal friction angle increased with the increase in displacement rate and was influenced by gradation and angularity. The friction angle for sand with angular, well-graded particles was higher than for sand with rounded, uniform particles. Rasti *et al.* (2021) studied the effect of particle size on the friction angle of soil through the DST and reported an increase in the friction angle as the coarse-grained

fraction in the soil increased. It was also established that for a higher uniformity coefficient, the friction angle was higher. Kang *et al.* (2022) studied the effect of moisture content and dry density on the shear strength of silty clay through DST. An increase in friction angle and cohesion was reported as dry density increased. The relationship curve between moisture content and the shear strength of the soil was found to be a concave quadratic curve. The shear strength and its parameters, cohesion and internal friction angle, all decreased with increased moisture content. Zhang *et al.* (2023) studied the variation in shear strength and its parameters by varying moisture content in different soil-rock mixtures. The cohesion, internal friction angle, and shear strength increased with gradual moisture content increase up to 12%. Beyond 12% water content, these magnitudes decreased. It can be observed from the discussed literature that such studies are mostly carried out on regular soils, with some experimental work reported for glacial tills. This study includes DST on reconstituted varved couplets, along with tests conducted on homogeneous samples. Nonetheless, the available studies on variation in shear strength parameters for samples subjected to different displacement rates at various moisture conditions are insufficient for a full understanding of the mechanisms.

Varved clays are a common type of laminated soil deposit in glacial environments, which are characterized by distinct, alternating light and dark-colored bands. Generally, the dark bands consist of clay-dominant laminae deposited in winter, whereas the light bands consist of silt-dominant laminae deposited in summer (Hang, 2003; Ehlers, 2022). These laminae result from the interaction between lake water turbulence, temperature, and the density distribution of sediment particles transported by moving and melting glaciers during summer. As winter begins and temperatures drop below freezing, glacier melting halts, glacier movement slows down, and no fresh debris is added to the lake. In still water conditions, the remaining fine particles from summer settle atop the coarser layer in the lake. This alternating settlement of coarse and fine particles creates a clear division, with visible light-colored and dark-colored laminae. Each pair of light and dark-colored bands forms a couplet, and their repetition over years creates deposits known as varves or varved clays (Lamoureux and Bradley, 1996; Lindqvist and Lee, 2009). The engineering properties of the two soils forming these laminae exhibit significantly different mechanical and infiltration responses under various stress conditions, making these soils inherently anisotropic (Leroueil *et al.*, 1990; Tankiewicz, 2015; Dobak *et al.*, 2018; Schneider *et al.*, 2022; Tornborg *et al.*, 2023; Philippe *et al.*, 2023). The darker lamina, which contains more clay-sized particles, has a higher natural moisture content in field conditions, lower hydraulic conductivity, higher plasticity, lower strength, and shows

greater volumetric changes under load than the lighter-colored lamina (Florkiewicz *et al.*, 2014; Flieger-Szymanska *et al.*, 2019). Despite these contrasting properties, the anisotropic behavior of varved clays is often overlooked due to the complexity of measuring various anisotropic parameters (Lacasse *et al.*, 1977). This study addresses this gap by investigating shear strength and its parameters through DST and comparing how the parameters for the varved couplet differ when considering its individual components. These individual components are treated as two separate samples that make up the homogeneous soil samples.

The present study uses two soils, Red Soil (RS) and Black Soil (BS). Three sets of samples are subjected to DST, including two homogeneous soil samples (RS and BS) and one reconstituted varved clay couplet. Reconstituted varved clay couplet samples are prepared with RS occupying the upper half volume of the shear box and BS the lower half. This RS-BS arrangement enables the determination of interface shear strength properties. RS and BS were selected based on laboratory geotechnical characterization to represent the laminae in actual varved clays. Glacier displacement rates can vary from nearly zero to 73 yr-1 (Paterson, 1994). In this study, to simulate glacial override, DST tests on samples are conducted at displacement rates of 1.25 mm/min, 0.24 mm/min, and 0.024 mm/min to analyze how shear strength responds to varying displacement rates. To simulate different glacial loads, the tests are conducted at normal stresses of 50 kPa, 100 kPa, and 150 kPa. Each soil sample undergoes DST testing in five moisture conditions, including dry, saturated, and unsaturated states with moisture contents at OMC, 0.8 OMC, and 1.2 OMC. Therefore, a total of 135 DST tests are conducted in this study. Although the behavior of soils in DST under different displacement rates and applied normal stresses offers a simplified simulation of how soils with varying compositions and moisture conditions may respond to different loads and loading rates, it is considered analogous in this study to varying glacial loads and velocities of glacial movement on soil.

2. Materials and Methodology

The two soils, RS and BS, used in this study were collected from in and around the IIT Guwahati campus. Preliminary geotechnical investigations were conducted to assess their suitability for replicating the soils that constitute the laminae of actual varved clays. Section 2.1 provides details on these geotechnical investigations, and Section 2.2 covers the methodology for sample preparation and execution of the testing series.

2.1 Material Characterization of RS and BS used as Constituent Laminae

Figure 1 shows the deposition sites of RS and BS, where the soils were collected. In the top-right corner of each site image, a close-up shows the soils in a tray after drying. In this dry and pulverized state, RS displays a coarser texture, while BS appears finer.

Figure 1. Representative samples of (a) RS and (b) BS collected in the vicinity of IIT Guwahati campus

Preliminary geotechnical investigations for selecting these soils included determining Atterberg limits (IS: 2720 Part 5-1985) and Particle Size Distribution (PSD) curves (IS: 2720 Part 4-1980), with the results listed in Table 1. The characteristics of RS and BS align with findings from Eden (1955), Kazi (1968), Eigenbrod and Burak (1991), Lydzba and Tankiewicz (2012), Florkiewicz *et al.* (2014), Tankiewicz (2016), Krawczyk and Szymanska (2018), and Flieger-Szymanska *et al.* (2019), indicating that RS is suitable for replicating the light-colored, silt-dominant laminae, while BS is suitable for the darker, clay-dominant laminae of actual varved clays. Table 1 also lists additional geotechnical parameters essential for assessing the engineering behavior of these soils, including specific gravity (IS: 2720 Part 3/Sec-2-1980) and compaction properties (IS: 2720 Part-7-1983).

Table 1. Geotechnical properties of RS and BS

Geotechnical Parameters	Red Soil (RS)	Black Soil (BS)
Specific Gravity	2.7	2.6
Atterberg Limit (%)		
Liquid Limit	45	95
Plastic Limit	19	30
Plasticity Index	26	65
Compaction Characteristics		
Dry Density	1.30	1.20
Maximum Dry Density (g/cc)	1.77	1.59
Optimum Moisture Content (%)	19.5	21.5
Grain Size Distribution (%)		
Sand	23.2	8.4
Silt	54.4	6.7
Clay	22.4	84.9
Soil Classification	ML	CH

Table 1 shows that RS and BS have liquid limits of 45% and 95%, respectively. The liquid limit magnitudes relate to the clay content in soil, with higher clay content yielding a higher liquid limit. Thus, the higher and lower liquid limits of BS and RS align with the clay content of 84.9% and 22.4%, as indicated in the PSD findings. Additionally, the plastic limits for RS and BS are 19% and 30%, respectively. The higher plastic limit of BS indicates that it requires more moisture to transition from a plastic to a semi-solid state, which suggests that BS retains moisture more effectively while remaining in a plastic state. The plasticity index of 26% for RS suggests moderate plasticity, while the high plasticity index of 65% for BS indicates a broader moisture range for plastic behavior. These differences in grain size and Atterberg limits between RS and BS result in distinct engineering behaviors when they form laminated soil structures, such as in varved clays.

2.1.1 Mineralogical and morphological characteristics of RS and BS

To verify that RS and BS represent soils similar to those found in the laminae of actual varved clays, apart from the above conducted geotechnical laboratory tests, X-ray Diffraction (XRD) and Field Emission Scanning Electron Microscopy (FESEM) analyses were conducted. Figures 2(a) and 2(b) display the XRD results, while Figures 3(a) and 3(b) present the FESEM findings for RS and BS. XRD analysis examines the crystal structures of the soil, while FESEM analysis focuses on microstructures of the soil. XRD involves illuminating the soil with X-rays and capturing the angles and intensities of the resultant scattered beams. In FESEM, electron beams

246 are used to create detailed images of the surface and topography of the soil through
247 electromagnetic lens focusing.
248
249 For the XRD analysis, RS and BS were finely ground and dried for 24 hours. The samples were
250 then placed on separate glass holders, gently pressed with a glass slide to create a smooth
251 surface, and any excess soil was removed. Removing excess soil is essential to ensure a smooth
252 sample surface for accurate XRD analysis. The prepared samples were placed in the XRD
253 instrument, where X-rays interacted with the crystal lattice of soil minerals to generate
254 diffraction patterns. These XRD patterns, shown in Figures 2(a) and 2(b), display peak
255 positions and intensities, which were compared to reference patterns in the literature to identify
256 the mineral composition of RS and BS. Results indicate that BS contains a significantly higher
257 amount of montmorillonite than RS. This finding is consistent with the work of Ringberg and
258 Erlström (1999), who reported similar results when separating and analyzing the summer
259 (lighter) and winter (darker) layers of varved clay. Blondeau (1975) also found that, while dark
260 and light laminae appeared mineralogically similar, the darker layers had a higher clay content,
261 primarily montmorillonite, while the lighter layers contained more illite with minor
262 montmorillonite. These observations align with the XRD results obtained for RS and BS in this
263 study.
264

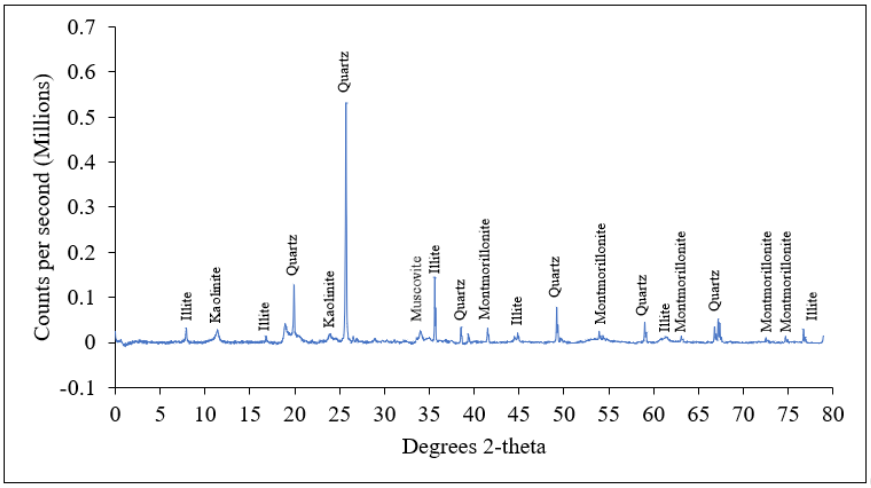

(a)

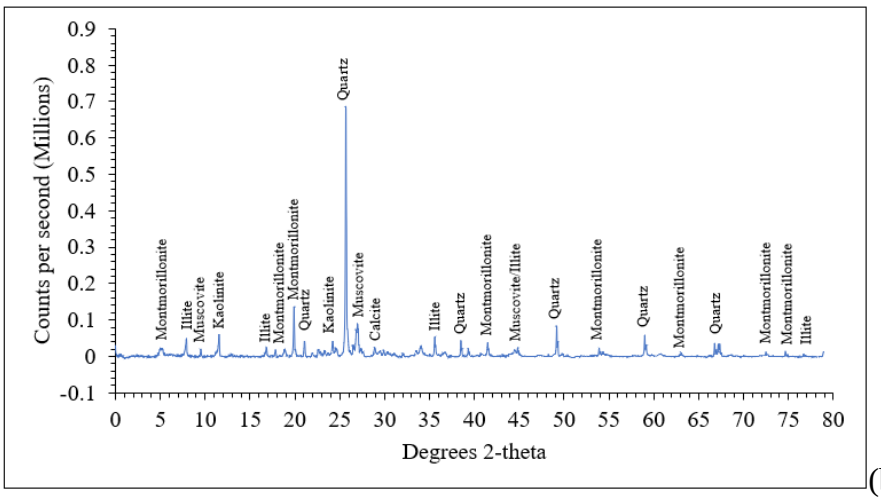

(b)

Figure 2. X-ray Diffraction spectra of (a) RS (b) BS samples

Figure 3 illustrates the microstructure of RS and BS obtained through FESEM analysis. FESEM requires more meticulous sample preparation than XRD. Both soils were finely ground and dried for 24 hours. Preparing samples for FESEM poses challenges, as soil samples may absorb atmospheric moisture during preparation and accumulate electric charges on the surface, which can result in blurred images and white patches. To minimize moisture exposure, the RS and BS samples were immediately sealed in an airtight container with silica beads after taking it out of oven. The samples were then mounted on a single stub with sticky carbon tape, and to prevent surface charging due to environmental moisture, these were gold-coated once positioned on the stub. This assembly of stubs and soil samples was then placed in the FESEM machine, and images were captured at 1000x magnification. The images revealed that RS particles are larger and more rounded (Figure 3a), while BS particles are flaky (Figure 3b), a typical shape for clay particles. Comparing the pore networks between particles, BS showed higher porosity than RS, likely due to the presence of clay minerals with a highly flocculated structure in BS, resulting in numerous inter-floc voids.

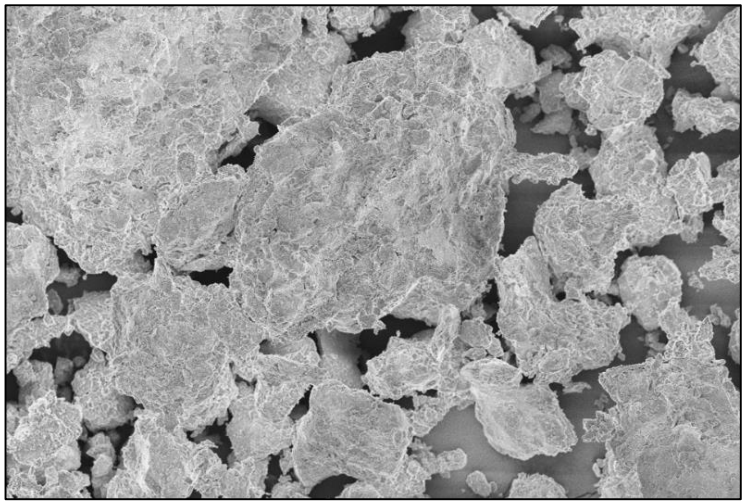

(a)

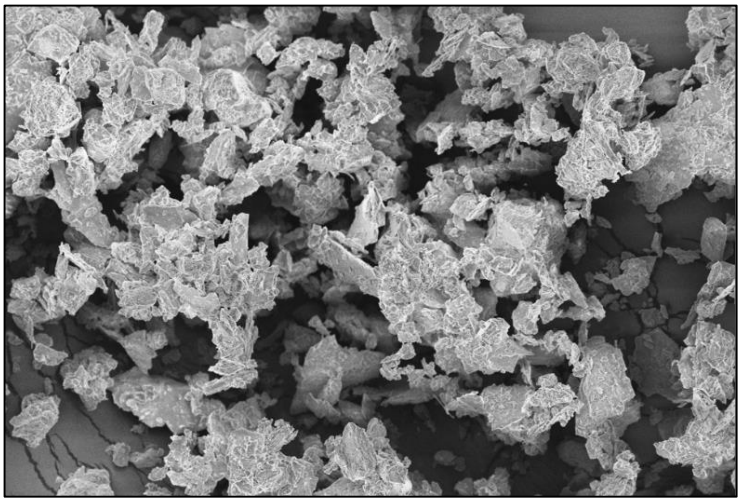

(b)

Figure 3. Field Emission Scanning Electron Microscopy (FE-SEM) showing microstructure of (a) RS (b) BS at 1000X magnification

Thus, in addition to the previously discussed geotechnical characteristics that indicate the suitability of RS and BS for replicating the soils constituting the laminae of varved clays, the mineralogical compositions and microstructures of these soils further support their suitability.

2.2 Methodology

The DST is conducted in accordance with ASTM D3080/D3080M (ASTM 2012). The samples prepared by weighing the soils based on their respective Maximum Dry Density (MDD), except for samples tested in a dry condition. For samples tested in a dry compacted state, weights are taken according to the dry density values listed in Table 1, which are 1.3 and 1.2 Mg/m^3 for RS and BS, respectively. The five moisture conditions at which the soils are compacted for DST preparation include dry and submerged conditions, along with three unsaturated states at water

content corresponding to OMC, 0.8 OMC, and 1.2 OMC. The MDD and OMC values, determined through the Standard Proctor Test (IS: 2720 Part-7-1983), are reported in Table 1 for both soils. RS has an MDD of 1.77 Mg/m³ and an OMC of 19.5%, while BS has an MDD of 1.59 Mg/m³ and an OMC of 21.5%. The lower OMC of RS is due to its higher sand and silt content, which allows for better packing and achieves MDD at a lower moisture content than BS. The higher OMC of BS is attributed to its high clay content, which requires more water for effective compaction.

Figure 4 presents the DST apparatus, including a zoomed-in view of a sample under submerged conditions. For testing samples under submerged conditions, each sample is first compacted at OMC within the direct shear box, and then the entire assembly is positioned in the DST apparatus. Weight loads are simultaneously applied according to the normal stresses required for the test. This setup prevents sample swelling and ensures accurate results. The soil is then submerged in water for 48 hours. During preparation for submerged DST, perforated grid metal plates are placed at the top and bottom of the sample, along with porous plates as shown in Figure 4(b), allowing water to percolate through the soil and fully saturate it. For all other samples prepared at the remaining moisture conditions, solid grid metal plates are used, as also shown in Figure 4(b).

The direct shear box used in this study has dimensions of 60 × 60 × 46 mm. However, the volume available for compacting the sample in the box is reduced due to the placement of various plates above and below the sample, as shown in Figure 4. For submerged conditions, the sample thickness is 28 mm, whereas for all other moisture conditions, the thickness is 33 mm. The same soil weight is used for all moisture conditions (based on MDD), except for samples tested in dry conditions.

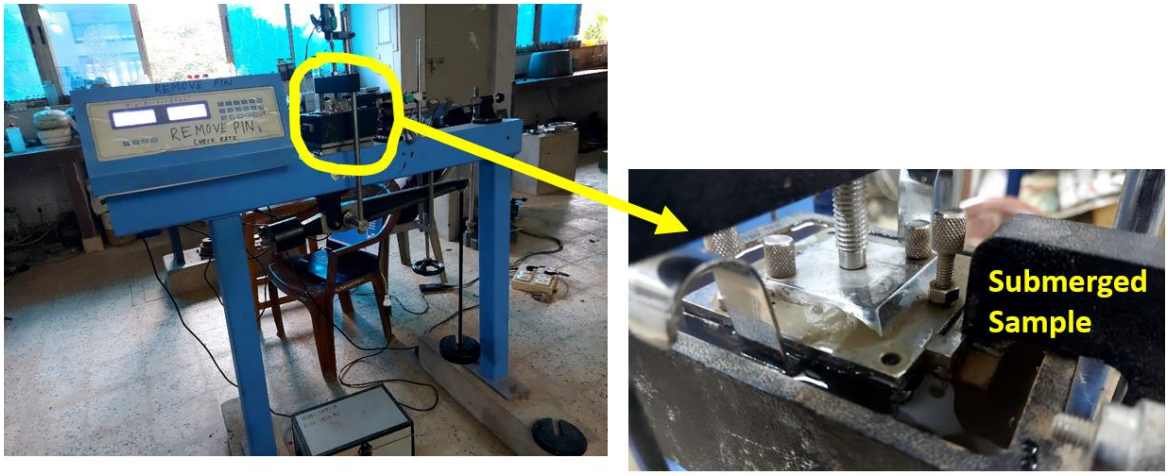

Figure 4(a). DST apparatus with a submerged soil sample

320

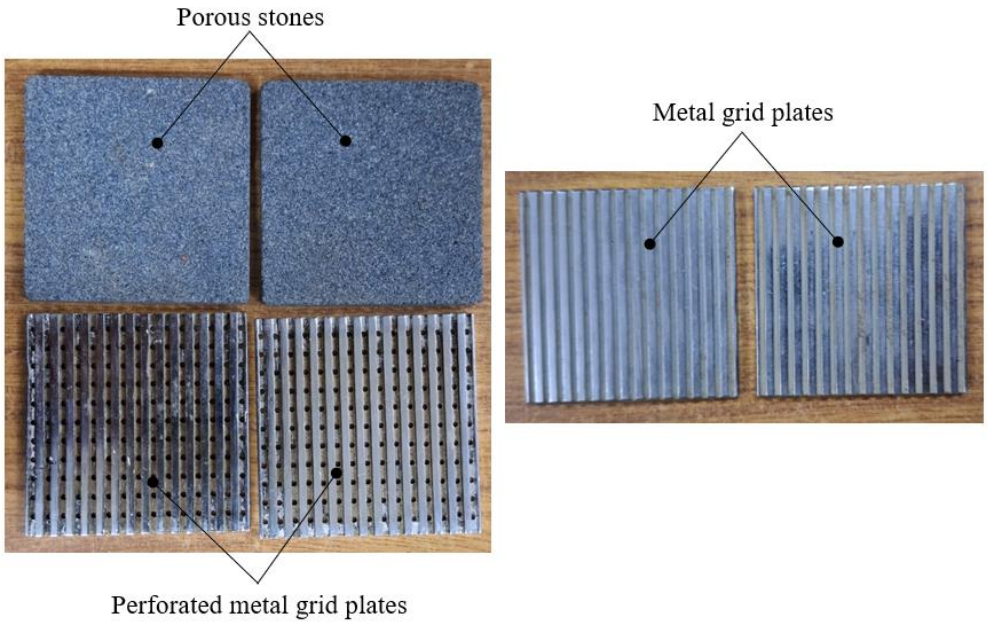

Figure 4(b). Metal grid plates and porous stones used in DST sample preparation

321

322 Homogeneous soil samples are prepared following standard DST sample preparation steps.
323 First, the required soil weight is calculated by multiplying the MDD by the volume of the direct
324 shear box. The weighed soil is then placed in a bowl and mixed to the designated moisture
325 content (OMC, 0.8 OMC, or 1.2 OMC). Before compacting the soil into the mold, a base plate
326 is placed in the shear box, followed by either a perforated plate and porous stone or solid grid
327 metal plates, depending on the moisture condition required for shearing as discussed earlier.
328 The soil sample is then compacted on top of this arrangement, followed by another perforated
329 plate and porous stone or solid grid metal plate, with the loading pad positioned on top. The
330 metal plates are arranged so that the grid lines are perpendicular to the applied shearing

direction. This entire assembly is then transferred to the direct shear apparatus for testing. A ball bearing is placed between the loading pad and the loading frame to ensure uniform stress distribution within the soil sample. Before beginning the test, it is essential to check that the lever arm is perfectly horizontal. Weights are then placed in the loading frame to apply normal stress to the soil sample, which is subsequently subjected to shearing at a specified displacement rate.

For the DST of reconstituted varved clay couplet samples, the placement of various plates during sample preparation and testing follows the same approach as discussed for homogeneous soil samples. However, for couplet samples, both RS and BS are used together in a direct shear box, with each soil weighed to correspond to half of the total volume required. RS and BS are weighed and taken in separate bowls and mixed with the required amount of water. The RS mixture is compacted into the lower half of the direct shear box, while the BS mixture is compacted into the upper half. This direct shear test method allows for the assessment of interface interaction between RS and BS in terms of shear strength and shear strength parameters.

Figure 5 presents a schematic diagram of compacted homogeneous soil samples in the direct shear box, where both the upper and lower halves contain the same soil. Figure 6(a) shows a schematic of reconstituted varved clay couplet samples in the direct shear box, with RS in the lower half and BS in the upper half. These figures also demonstrate the application of normal stress from the top of the sample and the horizontal displacement that moves the lower half of the direct shear box while the upper half remains stationary. Figure 6(b) illustrates the displacement of the lower box against the upper shear box, thereby generating shearing at the interface. In the DST, the failure plane is predefined and lies at the contact surface between the upper and lower boxes.

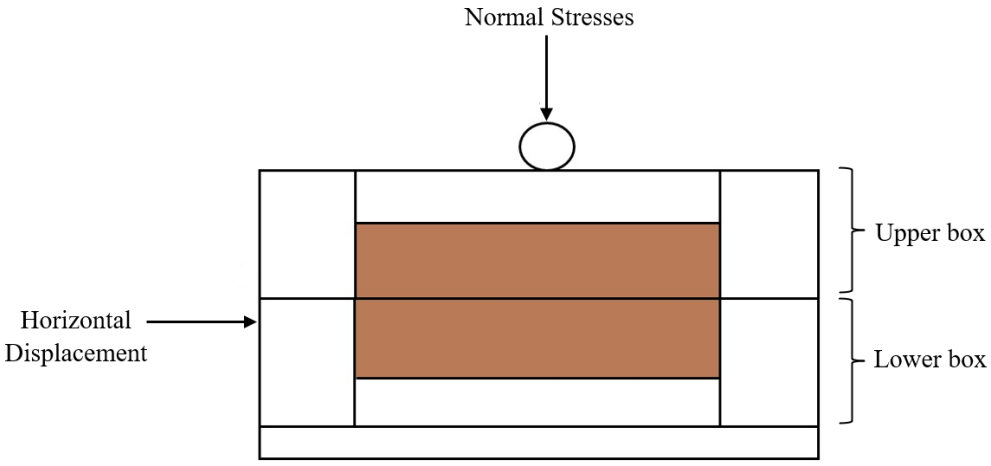

Figure 5. Schematic of homogeneous soil sample in a direct shear box showing application of normal load and direction of displacement

357

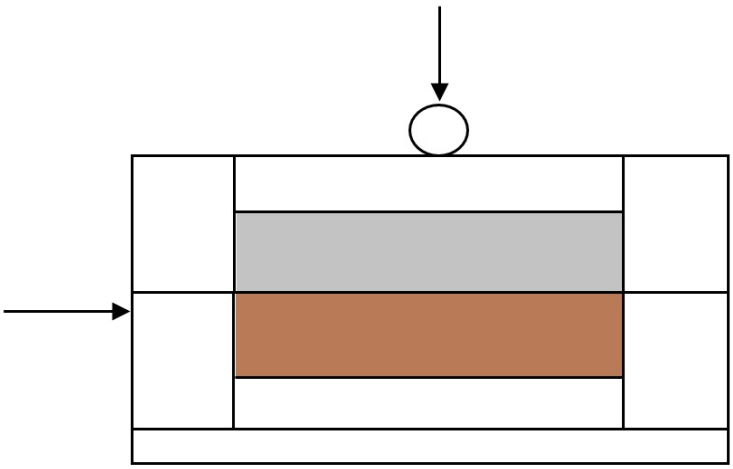

Figure 6(a). Schematic of reconstituted varve couplet in a direct shear box, showing layered configuration

358

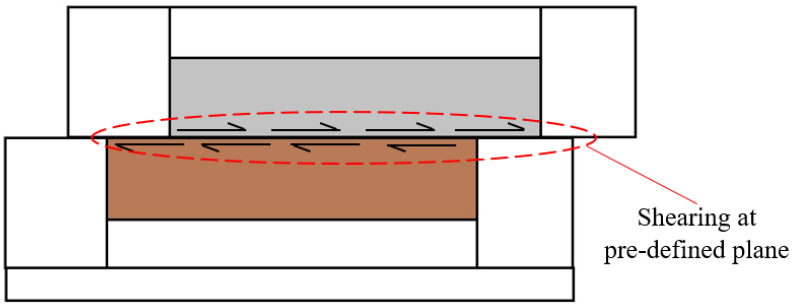

Figure 6(b). Schematic of reconstituted varve couplet in a direct shear box, illustrating shearing at the pre-defined plane at given horizontal displacement

359

In this study, it is hypothesized that glacial load and glacial override on soil are simulated by normal stresses and applied horizontal displacement rates, respectively, as discussed in Section 1. Each sample is tested under three normal stresses of 50 kPa, 100 kPa, and 150 kPa. Additionally, these soils, under various combinations of moisture conditions and normal stresses, are sheared at three horizontal displacement rates of 1.25 mm/min, 0.24 mm/min, and 0.024 mm/min.

3. Results and Discussion

This section discusses the variations in shear strength parameters—angle of internal friction and cohesion—and peak shear stresses at different applied normal stresses, displacement rates, and moisture contents in both homogeneous soils and reconstituted varved clay couplets.

In this study, the DST for different soil sample types is conducted under various combinations of moisture conditions and shearing displacement rates at three normal stresses of 50 kPa, 100 kPa, and 150 kPa. For each set of samples, the peak shear stresses at failure are plotted against the normal stresses, as demonstrated in Figure 7(a) for the reconstituted varved clay couplets sheared at a displacement rate of 0.024 mm/min and under different moisture conditions. From the graph, it is observed that at a particular moisture condition, as normal stress increases, the corresponding peak shear stress at failure increases linearly. The trend line for each set of shear-normal stress points is characterized by a unique intercept and slope, which represents the cohesion and angle of internal friction of the soil, respectively. Therefore, the trend line for each soil sample under different moisture and displacement rate combinations reflects the influence of these variables on the shear strength parameters of the soil.

The equation of the trend line in Figure 7(a) represents the relationship between peak shear stresses and normal stresses for each moisture condition. For the couplet sample compacted at a moisture condition of 0.8 OMC, the peak shear stresses at failure are the highest among all samples compacted at other moisture conditions and subjected to DST at a displacement rate of 0.024 mm/min. This same trend line for a moisture content of 0.8 OMC also shows the highest slope magnitude compared to all other tested samples under different moisture conditions. However, as the moisture content increases beyond 0.8 OMC, the peak shear stress magnitudes at given normal stresses decrease. Similarly, the angle of internal friction decreases as moisture content rises above 0.8 OMC, as indicated by the trend line slope. The lowest peak shear stress values at any normal stress are observed for samples tested under dry conditions. The observed increase in peak shear stresses with increasing normal stresses is consistent

across other reconstituted varved couplet samples sheared at displacement rates of 1.25 mm/min and 0.24 mm/min, as well as in all homogeneous RS and BS soil samples under all applied displacement rates and different moisture conditions. However, the variation in peak shear stresses at failure with normal stress is unique to each soil sample and its specific combination of these variables. Therefore, although the trend of the peak shear stress-normal stress plot remains the same for each sample set tested at the three applied normal stresses, the slopes and intercepts differ across cases. Thus, only one shear-normal stress graph is shown here (Figure 7a), while all obtained values are listed in Table 2.

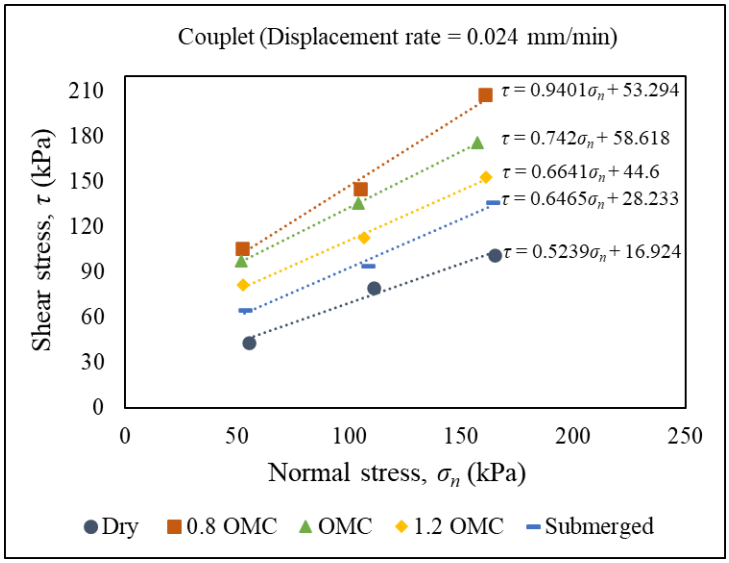

Figure 7 (a). Shear stress vs. normal stress plots for reconstituted varved couplets at different moisture conditions at 0.024 mm/min displacement rate

Figure 7(b) shows the peak shear stress vs. normal stress plots for reconstituted varved couplets prepared at a moisture content corresponding to OMC and sheared at displacement rates of 1.25 mm/min, 0.24 mm/min, and 0.024 mm/min under DST. The results indicate that peak shear stresses corresponding to the applied normal stresses are highest for the sample sheared at a displacement rate of 0.024 mm/min and decrease as the displacement rate increases. The equation of the trend line for each set of points at a given displacement rate further reveals that the slope and intercept magnitudes indicate an increase in the angle of internal friction and cohesion as the shearing displacement rate decreases. This trend is consistent for all combinations of soil samples and moisture contents, with only variations in the magnitudes of the outcome. Therefore, only one graph is shown here for illustrative purposes, with detailed information on different magnitudes included in Table 2. A detailed discussion of the angle of

internal friction, cohesion, and peak shear stresses at failure for different soils, moisture conditions, and displacement rates follows in the subsequent paragraphs.

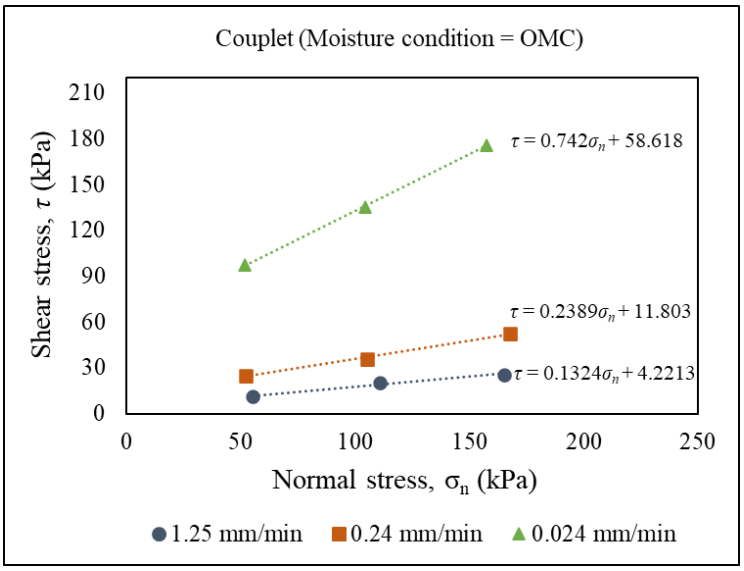

Figure 7(b). Shear stress vs. normal stress plots for reconstituted varved couplets at moisture content corresponding to OMC sheared at different displacement rates

Figures 8, 9, and 10 show the variation in the angle of internal friction and cohesion, for different moisture conditions at displacement rates of 1.25 mm/min, 0.24 mm/min, and 0.024 mm/min, respectively. It is observed from these figures that among the homogeneous RS and BS samples, the shear strength parameters are higher for homogeneous RS samples at the same moisture conditions and for a given displacement rate. The shear strength parameters for reconstituted varved clay couplets are observed to lie between the respective magnitudes of homogeneous RS and BS samples, with values generally closer to those of homogeneous BS samples.

Table 2. Shear strength for different soil samples at various displacement rates, moisture contents, and normal stresses

Moisture Condition = Dry					
	Displacement rates	**Normal stresses (σ_n)**	**50 kPa**	**100 kPa**	**150 kPa**
Shear strength (τ_{max})	**1.25 mm/min**	**RS**	7.6	12.2	18.9
		BS	4.4	8.6	11.8
		Couplet	7.8	11.8	20.4
	0.24 mm/min	**RS**	10.0	16.1	23.6
		BS	5.6	10.0	14.3
		Couplet	12.5	20.0	32.8
	0.024 mm/min	**RS**	60.2	111.3	157.4
		BS	36.3	60.2	86.0
		Couplet	43.6	80.8	101.1
Moisture Condition = 0.8 OMC					
	Displacement rates	**Normal stresses (σ_n)**	**50 kPa**	**100 kPa**	**150 kPa**
Shear strength (τ_{max})	**1.25 mm/min**	**RS**	24.1	39.0	54.3
		BS	11.9	19.0	25.8
		Couplet	12.2	21.5	31.7
	0.24 mm/min	**RS**	35.4	51.2	72.8
		BS	18.4	25.0	34.3
		Couplet	20.8	31.6	49.1
	0.024 mm/min	**RS**	154.0	235.9	285.9
		BS	95.6	136.0	170.9
		Couplet	105.9	145.6	207.6
Moisture Condition = OMC					
	Displacement rates	**Normal stresses (σ_n)**	**50 kPa**	**100 kPa**	**150 kPa**
Shear strength (τ_{max})	**1.25 mm/min**	**RS**	25.3	43.7	63.9
		BS	12.0	21.3	30.0
		Couplet	11.0	20.1	25.5
	0.24 mm/min	**RS**	33.5	49.9	70.7

		BS	17.9	30.4	42.3
		Couplet	25.0	35.9	53.0
	0.024 mm/min	**RS**	175.7	256.4	368.6
		BS	94.1	161.4	209.9
		Couplet	97.4	136.2	177.0

Moisture Condition = 1.2 OMC

	Displacement rates	**Normal stresses (σ_n)**	**50 kPa**	**100 kPa**	**150 kPa**
Shear strength (τ_{max})	**1.25 mm/min**	**RS**	12.6	18.2	29.9
		BS	9.0	15.6	22.1
		Couplet	9.3	16.7	24.0
	0.24 mm/min	**RS**	21.9	31.8	44.0
		BS	14.1	19.4	29.6
		Couplet	18.3	32.2	43.7
	0.024 mm/min	**RS**	104.8	144.9	199.7
		BS	57.4	93.4	125.7
		Couplet	81.6	112.2	153.8

Moisture Condition = Submerged

	Displacement rates	**Normal stresses (σ_n)**	**50 kPa**	**100 kPa**	**150 kPa**
Shear strength (τ_{max})	**1.25 mm/min**	**RS**	9.1	14.9	21.1
		BS	6.7	12.3	20.0
		Couplet	9.9	15.0	24.7
	0.24 mm/min	**RS**	13.8	21.6	28.2
		BS	9.8	18.5	23.8
		Couplet	14.7	25.3	39.5
	0.024 mm/min	**RS**	76.0	109.3	138.8
		BS	45.5	70.3	100.0
		Couplet	65.1	94.2	136.3

Figures 8(a), 9(a), and 10(a) show the variation of the angle of internal friction for different soil samples under different moisture conditions, with samples sheared at displacement rates of 1.25 mm/min, 0.24 mm/min, and 0.024 mm/min, respectively. Among the homogeneous RS

and BS samples, the angle of internal friction is consistently higher for RS than for BS under similar moisture conditions tested under DST at a given displacement rate. This high friction angle in homogenous RS samples can be attributed to its grain size composition and low plasticity index (Table 1). The particle composition of RS includes significant portions of both sand and silt, which results in a denser, more interlocked structure upon compaction compared to BS under similar moisture conditions. For BS, particle interlocking is hindered due to a high percentage of clay-sized particles and higher plasticity. In high clay content soils, such as BS, clay minerals tend to absorb and retain more moisture, due to which a thick film of water gets formed around soil particles. This water film acts as a lubricant between the soil grains, and prevents the formation of interparticle locking in BS. Consequently, the angle of internal friction for BS is consistently lower than for RS under similar moisture conditions and displacement rates. In both homogeneous RS and BS samples, the angle of internal friction initially increases from dry conditions, peaks at OMC, and then decreases until saturation. This trend suggests that increasing moisture content in soils enhances particle interlocking up to OMC, which results in an increased friction angle. Beyond OMC, additional water in soil acts as a lubricant, which weakens the interparticle friction and reduces the friction angle magnitudes in both the soils. However, the rate at which the friction angle changes with varying moisture conditions differs between RS and BS samples. Both the rates of increase and decrease in the angle of internal friction with moisture conditions are higher for RS compared to BS. This is evident from the steeper curve for RS as moisture conditions change, while the curve for BS is relatively gradual. RS is thus more sensitive to changing moisture conditions than BS. Due to this difference in sensitivity, the gap between the friction angle curves for RS and BS widens up to OMC, and then gradually narrows down toward the submerged moisture condition. This trend is observed for all displacement rates, with the friction angle difference between homogeneous RS and BS samples being greatest at 1.25 mm/min, followed by 0.24 mm/min, and then 0.024 mm/min. For reconstituted varved clay couplets, the maximum angle of internal friction is achieved at a moisture content corresponding to 0.8 OMC, unlike the homogeneous samples, which reach their peak friction angle at OMC. The friction angle for the couplet samples is higher than for both homogeneous RS and BS profiles under dry and submerged conditions. Additionally, the rate of decrease in the friction angle is very gradual for the couplet samples from OMC to submerged conditions, as evident from the nearly horizontal curve between these moisture conditions. These observations hold true for all displacement rates. Lastly, it is observed from these figures that as the displacement rate decreases, the angle of internal friction increases for all soil samples, including homogeneous

RS, homogeneous BS, and reconstituted varved clay couplets, under a given moisture condition. This increase in friction angle with decreasing displacement rate is attributed to the additional time available for soil grains to adjust and rearrange at lower displacement rates, which maximizes the interlocking and provides higher resistance to shearing.

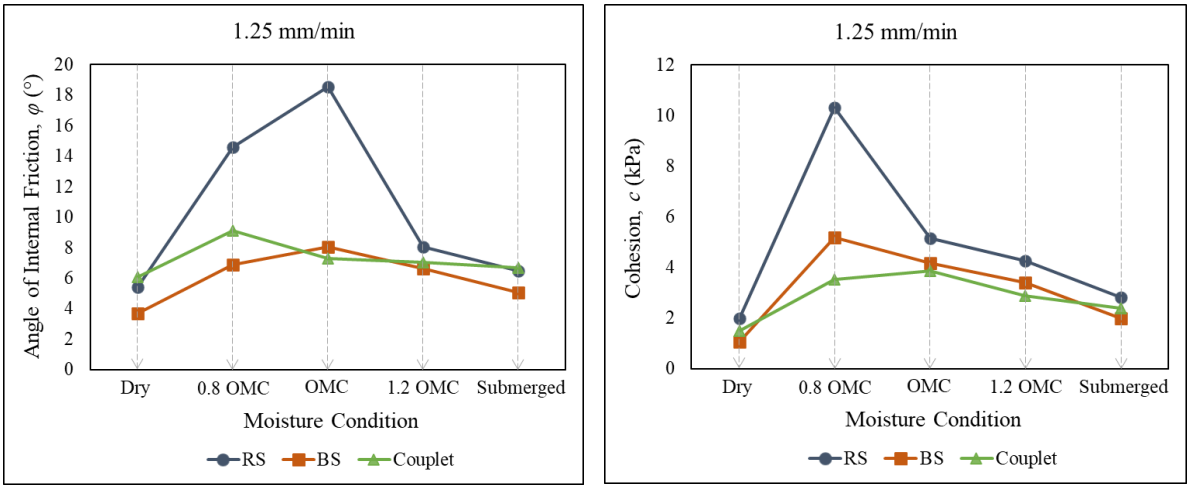

(a) (b)

Figure 8. Variation in shear strength parameters (a) Angle of Internal Friction and (b) Cohesion at a displacement rate of 1.25 mm/min across different moisture conditions

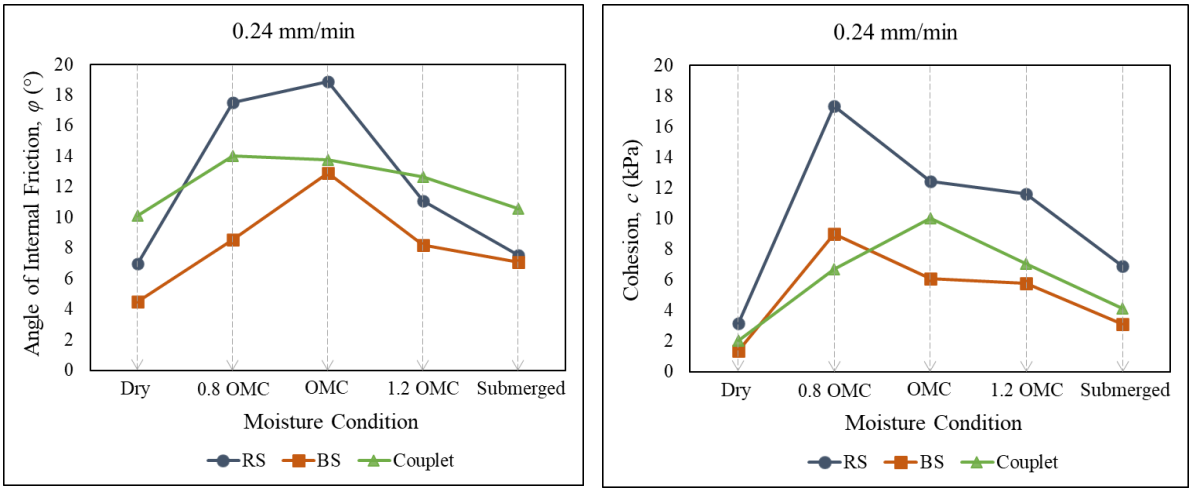

(a) (b)

Figure 9. Variation in shear strength parameters (a) Angle of Internal Friction and (b) Cohesion at a displacement rate of 0.24 mm/min across different moisture conditions

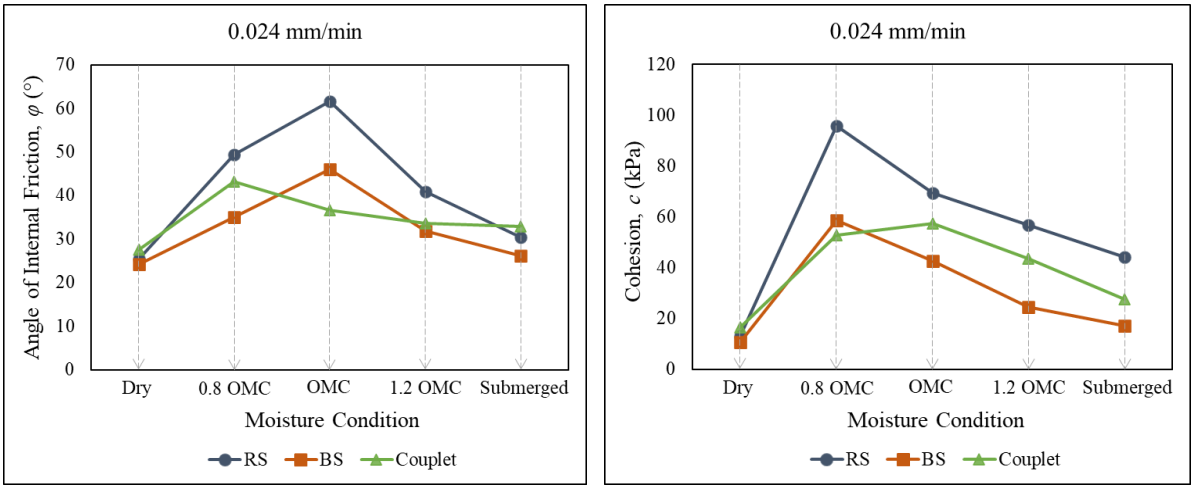

(a) (b)

Figure 10. Variation in shear strength parameters (a) Angle of Internal Friction and (b) Cohesion at a displacement rate of 0.024 mm/min across different moisture conditions

Figures 8(b), 9(b), and 10(b) show the variation of cohesion at different moisture conditions for different soil samples sheared at displacement rates of 1.25 mm/min, 0.24 mm/min and 0.024 mm/min, respectively, under DST loading. Similar to the behavior observed for the angle of internal friction, the cohesion values are higher for homogeneous RS samples compared to homogeneous BS samples under similar moisture conditions and displacement rates. The cohesion increases from samples tested in dry conditions, peaks for samples compacted at 0.8 OMC, and then decreases as moisture content increases up to submerged conditions. Notably, even though RS has a lower clay content than BS, its cohesion values are higher, which can be attributed to higher apparent cohesion. Apparent cohesion refers to cohesive behavior typically observed in unsaturated soils. It differs from true cohesion, which involves molecular-level attraction between soil particles, such as Van der Waals forces. In this scenario, the ability of RS to compact to a higher density due to its particle size distribution results in smaller pore spaces compared to those in BS, which allows for the development of stronger capillary forces in RS, which, in turn, leads to higher cohesion in RS compared to BS. For reconstituted varved clay couplets subjected to different displacement rates, maximum cohesion is observed in samples prepared at a water content corresponding to OMC. Additionally, the cohesion of couplet samples is higher than that of homogeneous BS samples under dry and submerged conditions. However, for unsaturated states, the cohesion magnitude in the couplet is less than that of BS for all displacement rates. Similar to homogeneous soil samples, the cohesion in the reconstituted couplet also increases with a decrease in displacement rate. Table 3 provides the exact values for the friction angle and cohesion corresponding to the trends observed in Figures

8, 9, and 10. From these observations, it can be concluded that both the angle of internal friction and cohesion are not intrinsic properties of the soil. These shear strength parameters vary with moisture content and the displacement rate at which the soil is sheared. Therefore, the derived shear strength parameters—cohesion and friction angle obtained through laboratory tests are referred to as apparent cohesion and apparent friction angle.

Table 4 shows the rate of increase in the magnitudes of the angle of internal friction and cohesion for different soil samples (RS, BS, and reconstituted varved couplet) at various moisture conditions when the displacement rate in the DST test is reduced. The table presents the number of folds by which the shear strength parameters increase as the displacement rate is reduced from 1.25 mm/min to 0.24 mm/min and from 1.25 mm/min to 0.024 mm/min. The rate of increase is significantly higher when the displacement rate changes from 1.25 mm/min to 0.024 mm/min compared to the change from 1.25 mm/min to 0.24 mm/min. Additionally, it is observed that the magnitude of cohesion is more sensitive to changes in displacement rate than the angle of internal friction, as indicated by the higher rate of increase in cohesion compared to the rate of increase in the friction angle for a given soil sample at a specific moisture condition.

Table 3. Rate of Increase in shear strength parameters for different soil profiles at various moisture contents with variation in displacement rate

Moisture condition	**Dry**		**0.8 OMC**		**OMC**		**1.2 OMC**		**Submerged**	
Shear strength parameters	ϕ	c	ϕ	c	ϕ	c	ϕ	c	ϕ	c
0.024 mm/min										
RS	25.5	13.3	49.3	95.8	61.7	69.5	41.0	56.8	30.5	44.1
BS	24.2	10.7	35.0	58.5	46.0	42.6	31.8	24.6	26.2	17.2
Couplet	27.6	16.6	43.2	52.9	36.6	57.5	33.6	43.7	32.9	27.7
0.24 mm/min										
RS	7.0	3.2	17.5	17.4	18.9	12.4	11.1	11.6	7.5	6.9
BS	4.5	1.4	8.6	9.0	12.9	6.1	8.2	5.8	7.1	3.1
Couplet	10.1	2.1	14.0	6.7	13.8	10.0	12.7	7.1	10.6	4.1
1.25 mm/min										
RS	5.4	2.0	14.6	10.3	18.6	5.2	8.0	4.3	6.5	2.8
BS	3.7	1.1	6.9	5.2	8.0	4.2	6.6	3.4	5.1	2.0
Couplet	6.1	1.5	9.1	3.5	7.3	3.9	7.0	2.9	6.7	2.4

Table 4. Rate of increase in shear strength parameters for different soil profiles at various moisture contents with variation in displacement rate

Moisture condition	**Dry**		**0.8 OMC**		**OMC**		**1.2 OMC**		**Submerged**	
Rate of increase in shear strength parameters	ϕ	c	ϕ	c	ϕ	c	ϕ	c	ϕ	c
1.25 mm/min to 0.24 mm/min										
RS	1.29	1.59	1.20	1.68	1.02	2.41	1.38	2.72	1.16	2.46
BS	1.22	1.26	1.25	1.73	1.61	1.46	1.23	1.71	1.39	1.57
Couplet	1.66	1.37	1.54	1.89	1.88	2.58	1.81	2.44	1.58	1.72
1.25 mm/min to 0.024 mm/min										
RS	4.72	6.63	3.38	9.29	3.32	13.47	5.10	13.30	4.71	15.67
BS	6.59	9.92	5.10	11.26	5.73	10.22	4.79	7.25	5.15	8.60
Couplet	4.54	11.07	4.75	14.97	5.01	14.84	4.79	15.11	4.91	11.54

Figures 11, 12, and 13 show the variation in peak shear stresses at failure for different samples subjected to DST under various moisture conditions and applied normal stresses, tested at displacement rates of 1.25 mm/min, 0.24 mm/min, and 0.024 mm/min, respectively. These figures indicate that as the applied normal stress on the sample increases, the corresponding peak stresses at failure also increase, as observed in Figure 7. Additionally, the figures demonstrate that increasing moisture content in the samples up to a certain limit yields maximum peak stresses at failure. The increase in peak shear stresses with applied normal stresses can be attributed to the enhanced confinement of the soil sample in the direct shear box as normal stress increases. Enhanced confinement due to increased loading restricts the movement of soil particles in the shear box and increases the contact area between particles during shearing. This denser particle arrangement at higher normal stresses not only improves interparticle friction and apparent cohesion but also prevents dilation or separation of soil particles, which provides greater resistance to applied horizontal shearing forces at a given displacement rate. Therefore, the soil exhibits higher resistance to shearing under higher normal stresses, resulting in higher peak shear stresses at failure. It is also observed that, for all soil samples sheared at different displacement rates and subjected to various normal stresses, the shear strength generally peaks for samples compacted at moisture contents around the OMC or 0.8 OMC and then decreases as moisture content approaches saturation (submerged conditions). This suggests that an initial increase in moisture enhances apparent cohesion and friction angle up to a certain threshold, resulting in increased shear strength. Beyond this moisture threshold, excess water acts as a lubricant, reducing these shear strength parameters and, consequently, the overall shear strength.

Figures 11, 12, and 13 further show that, at displacement rates of 1.25 mm/min and 0.024 mm/min, the peak shear stress for homogeneous RS and BS samples occurs at water content corresponding to the OMC for all applied normal stresses. This suggests that homogenous RS and BS samples prepared at OMC for DST, provides an optimal balance of water that promotes particle cohesion and interlocking, leading to the highest resistance against shear forces. However, in the reconstituted varved clay couplet sheared at these rates, peak shear stresses are observed for the samples prepared at a slightly lower moisture level of 0.8 OMC. This finding indicates that the interface shear properties of RS and BS layers within the couplet reach maximum shear stresses at failure at a slightly drier condition than OMC. This result likely arises from a greater influence of the angle of internal friction over cohesion at these displacement rates, as similar trends have been observed for friction angles between homogeneous and couplet samples (Figures 8 and 10).

At the intermediate displacement rate of 0.24 mm/min (Figure 9), the moisture content at which peak shear stresses are achieved differs from observations at the other two displacement rates, 1.25 mm/min and 0.024 mm/min. In homogeneous RS samples, peak shear stresses occur under DST at a water content corresponding to 0.8 OMC, while for homogeneous BS and the reconstituted couplet, peak shear stresses are reached for samples prepared at OMC for all normal stresses. This difference suggests that, at the intermediate displacement rate, the homogeneous RS sample, which has a higher sand and silt content, achieves an optimal combination of interparticle friction and cohesion at a slightly lower moisture content than the other two samples subjected to DST. These observations demonstrate that when soil is sheared at different normal stresses, its composition and structure significantly affected by the moisture content at which the peak stresses at failure is achieved, which further varies with the applied displacement rate.

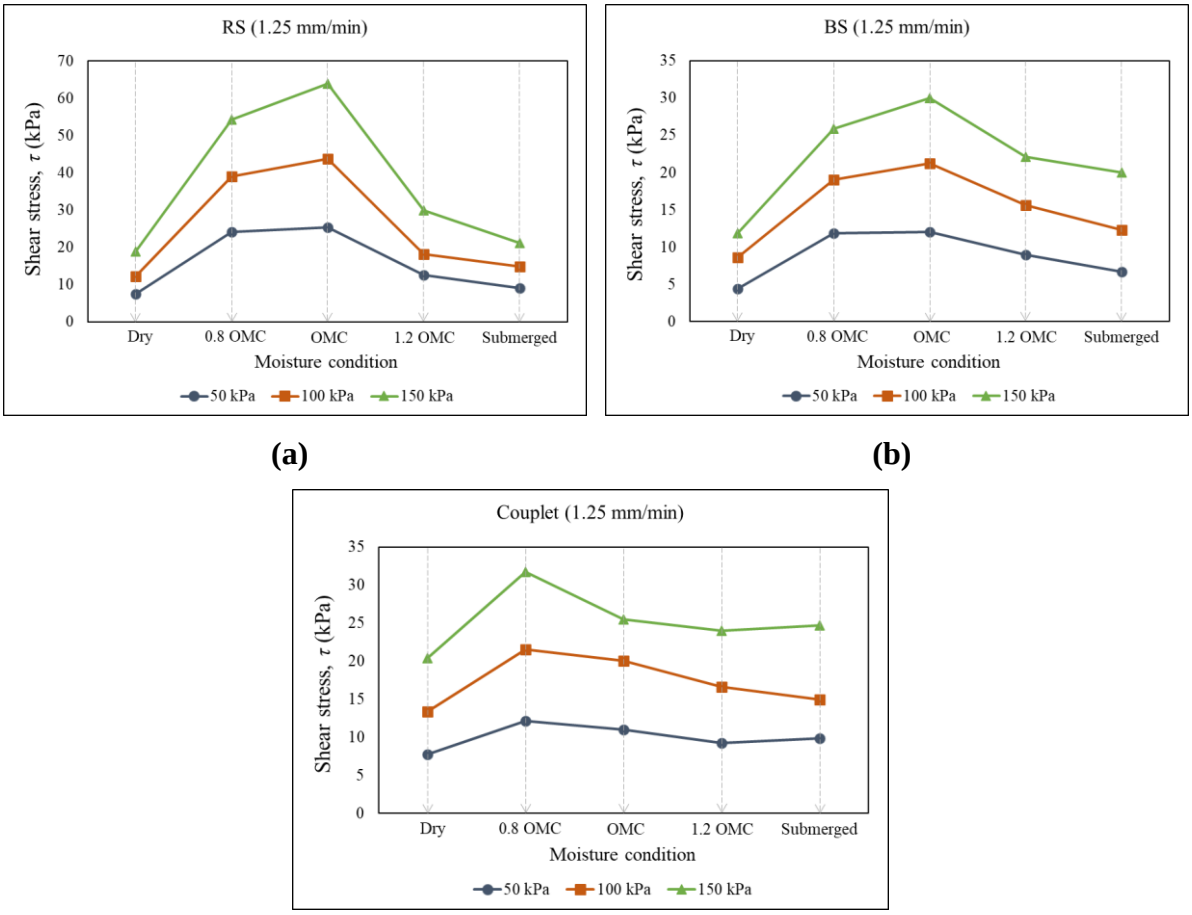

Figure 11. Variation in shear strength with moisture conditions at displacement rate of 1.25 mm/min for (a) Homogeneous RS, (b) Homogeneous BS, and (c) Reconstituted varved couplet

572

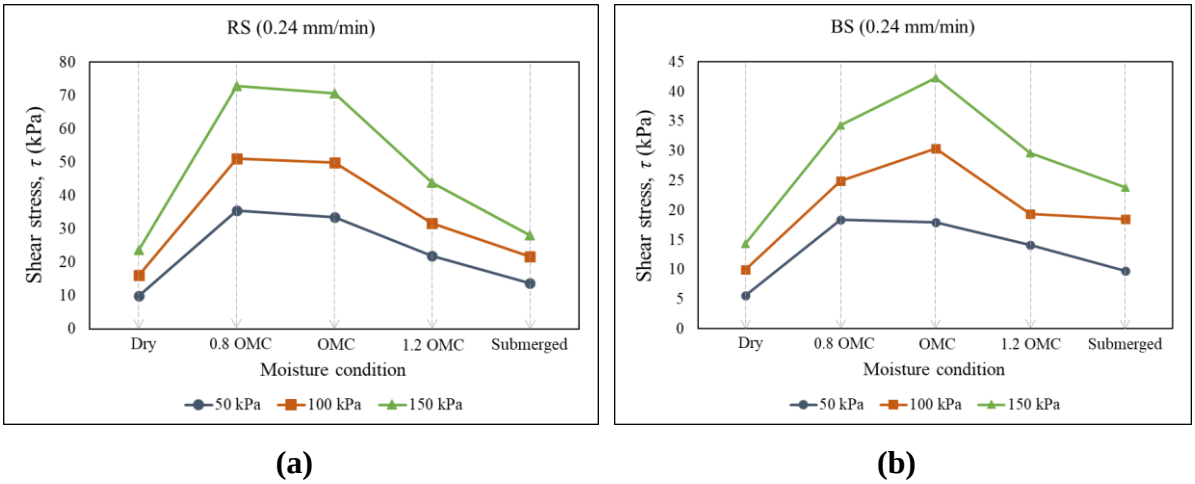

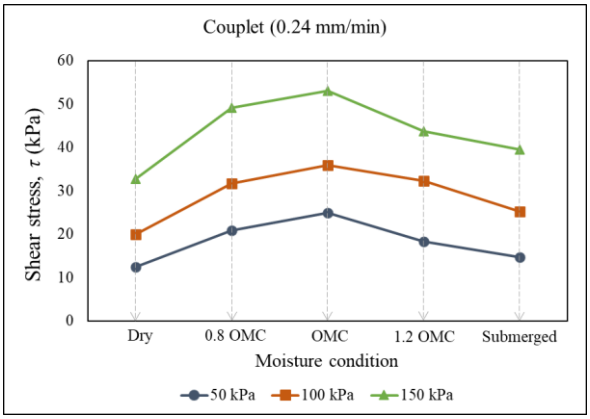

(c)

Figure 12. Variation in shear strength with moisture conditions at displacement rate of 0.24 mm/min for (a) Homogeneous RS, (b) Homogeneous BS, and (c) Reconstituted varved couplet

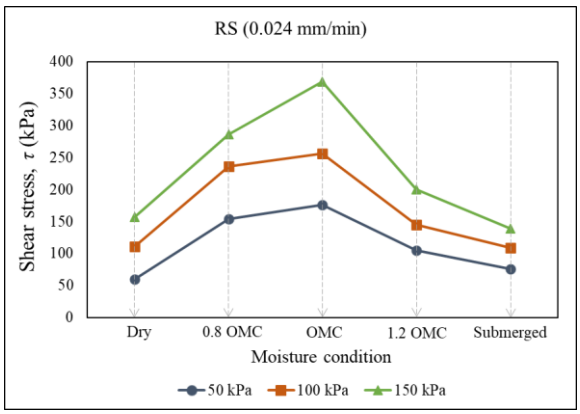

(a)

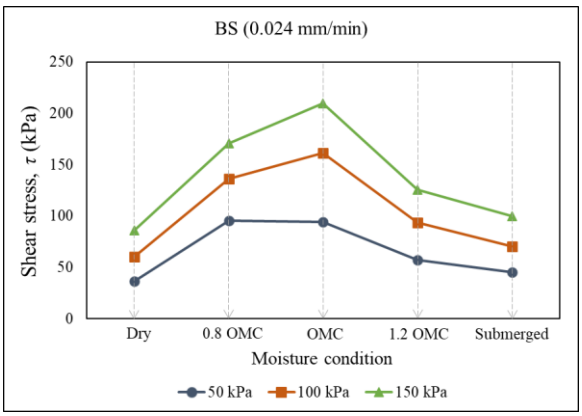

(b)

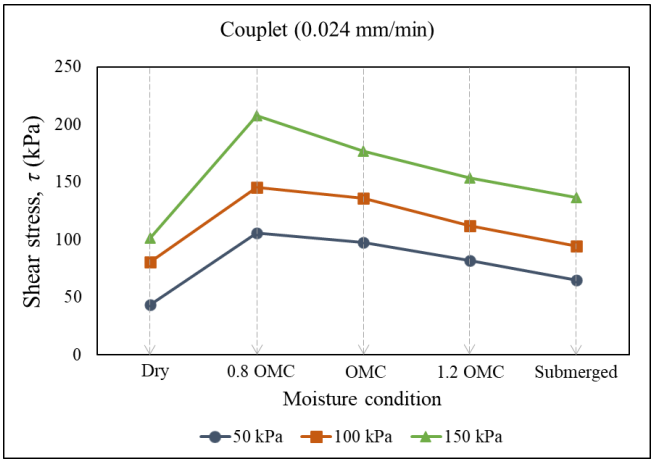

(c)

Figure 13. Variation in shear strength with moisture conditions at displacement rate of 0.024 mm/min for (a) Homogeneous RS, (b) Homogeneous BS, and (c) Reconstituted varved couplet

The DST is conducted on each soil sample at specific moisture content and displacement rate under three applied normal stresses of 50 kPa, 100 kPa, and 150 kPa. DST on soil samples from each combination of these variables yields a unique stress-displacement curve. Figures 14, 15, 16, 17, and 18 present the shear stress-displacement curves from DST for RS, BS, and the reconstituted varved couplet, showing responses under different combinations of these values at applied normal stresses. These figures show that for soil samples prepared at the same moisture condition and subjected to the same displacement rate, the shear stress-displacement curve shifts upward, and the peak shear stress occurs at higher displacement magnitudes as normal stress increases. This behavior of the stress-displacement curve likely results from the enhanced confinement effect as normal stress increases, as discussed in preceding paragraphs. Enhanced confinement restricts particle movement within the shear box, pressing particles more tightly together, which leads to higher resistance against horizontal shearing as normal stress increases. This increased resistance to shearing shifts the stress-displacement curve upward. Additionally, because particles are more tightly confined under higher normal stresses, more displacement is needed for the soil sample to fully mobilize and allow particles to slide against each other, causing peak shear stress to occur at higher displacement values. For example, Figure 14 shows that the peak shear stress for the homogeneous RS sample occurs at displacement magnitudes of 3 mm, 4 mm, and 4.5 mm for normal stresses of 50 kPa, 100 kPa, and 150 kPa, respectively. For the homogeneous BS sample, the corresponding displacement magnitudes at these normal stresses are 4.1 mm, 5.6 mm, and 6.3 mm, while for the reconstituted varved couplet, the displacement magnitudes are 5.2 mm, 5.8 mm, and 6 mm.

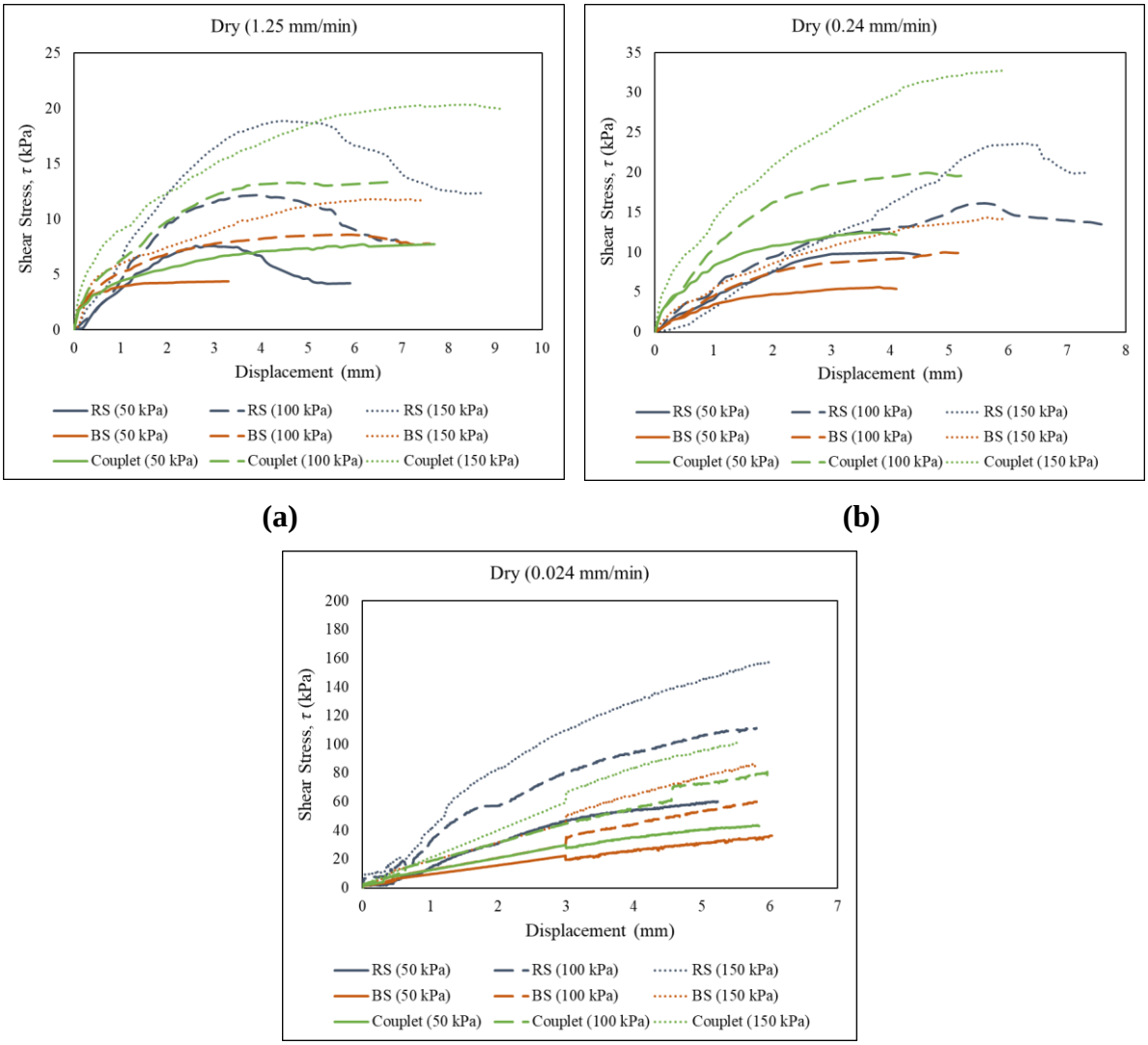

Figure 14. Variation in shear strength of different soil samples compacted in dry conditions with horizontal displacement at applied normal stresses and displacement rates of (a) 1.25 mm/min, (b) 0.24 mm/min, and (c) 0.024 mm/min

601

602

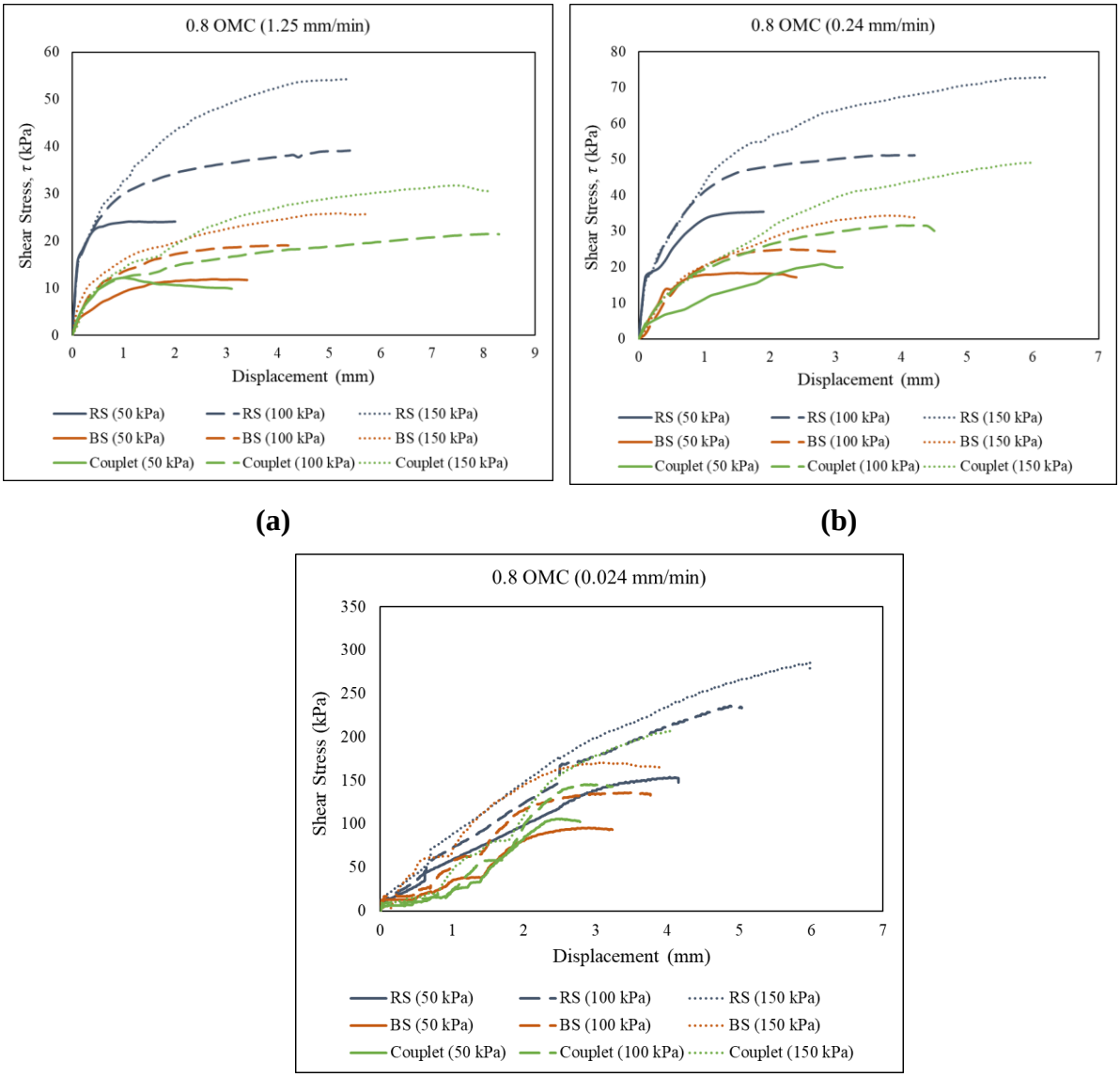

Figure 15. Variation in shear strength of different soil samples compacted at 0.8 OMC moisture content with horizontal displacement at applied normal stresses and displacement rates of (a) 1.25 mm/min, (b) 0.24 mm/min, and (c) 0.024 mm/min

603

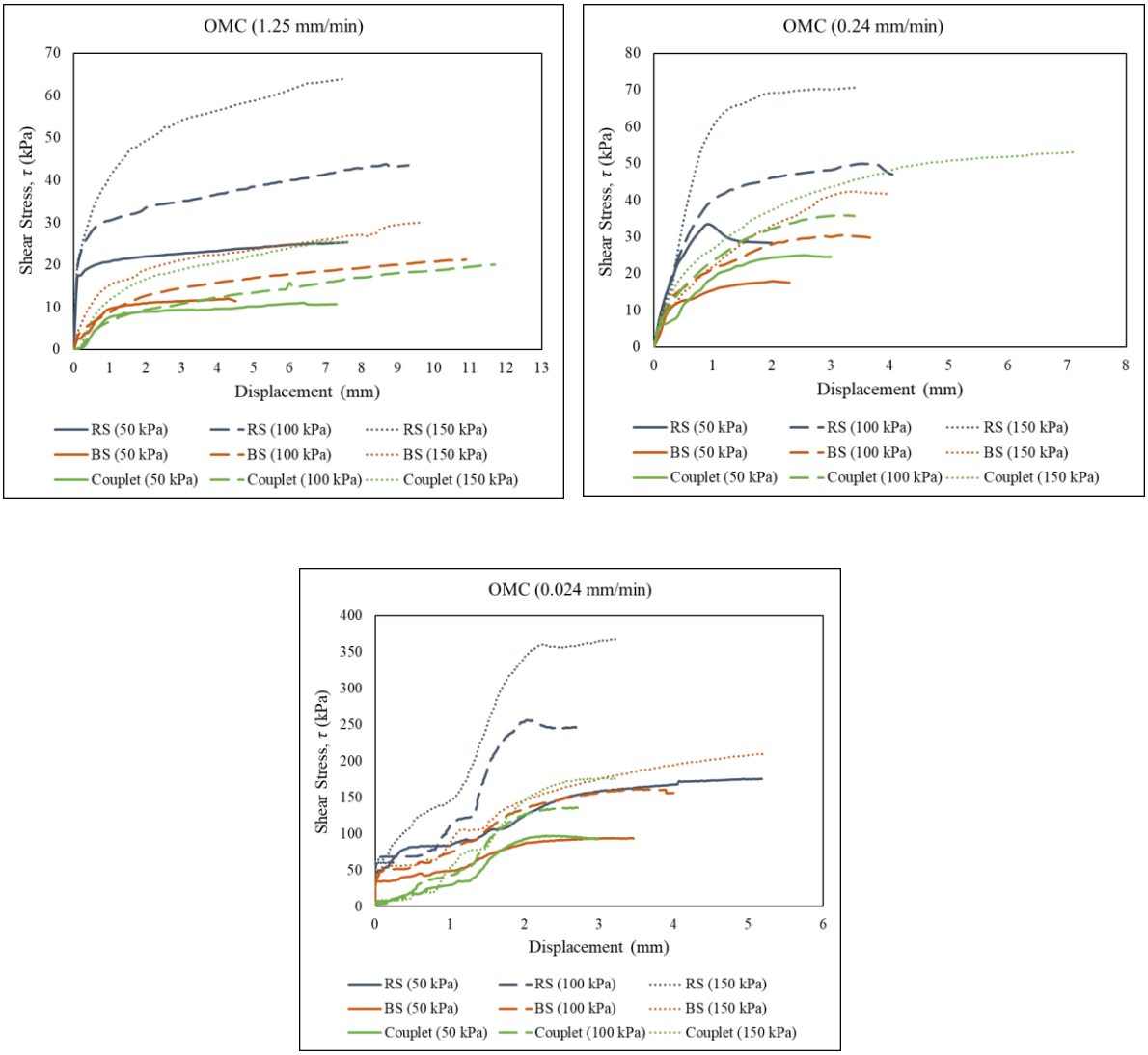

Figure 16. Variation in shear strength of different soil samples compacted at OMC moisture content with horizontal displacement at applied normal stresses and displacement rates of (a) 1.25 mm/min, (b) 0.24 mm/min, and (c) 0.024 mm/min

604

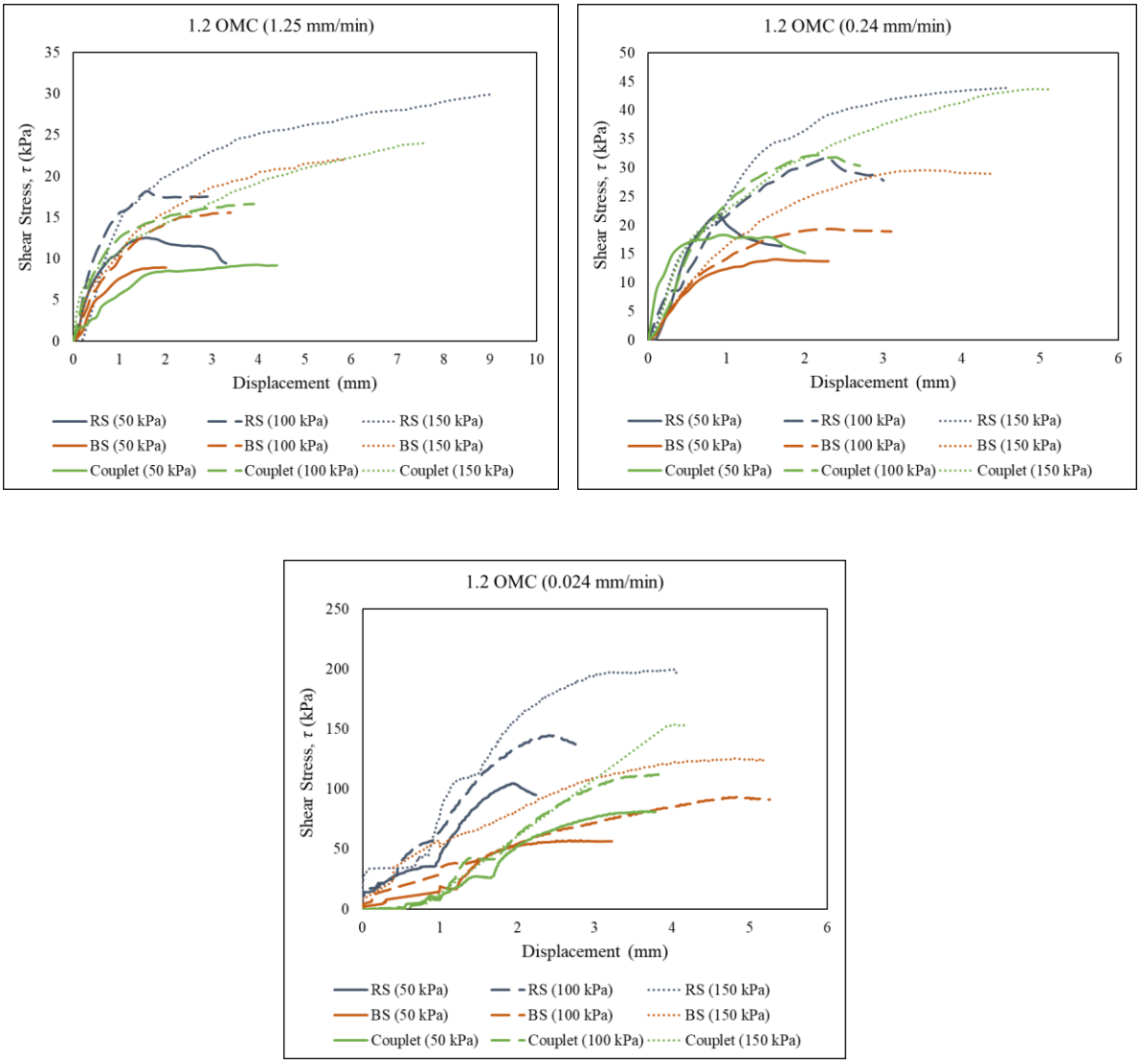

Figure 17. Variation in shear strength of different soil samples compacted at 1.2 OMC moisture content with horizontal displacement at applied normal stresses and displacement rates of (a) 1.25 mm/min, (b) 0.24 mm/min, and (c) 0.024 mm/min

605

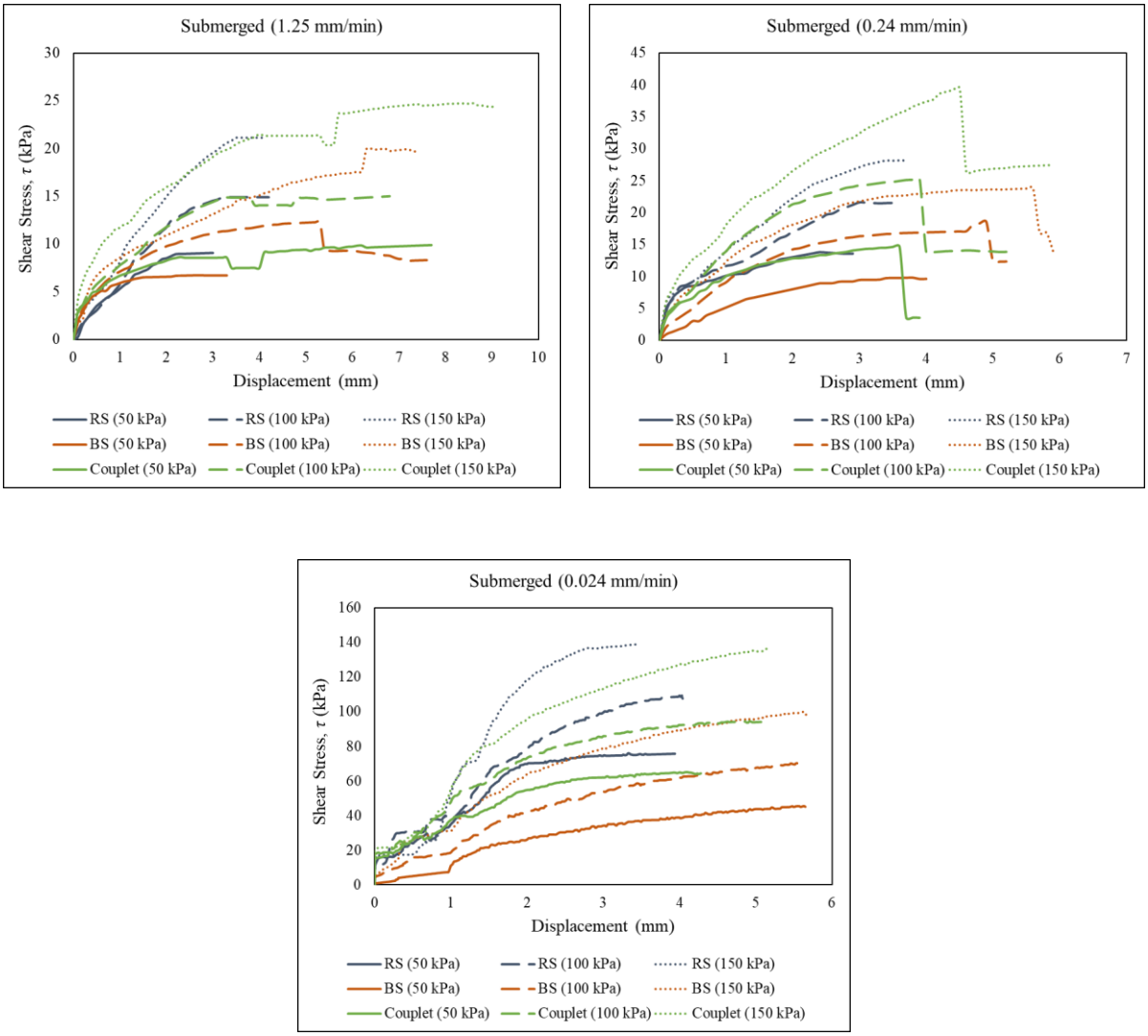

Figure 18. Variation in shear strength of different soil samples in submerged conditions with horizontal displacement at applied normal stresses and displacement rates of (a) 1.25 mm/min, (b) 0.24 mm/min, and (c) 0.024 mm/min

606

607 A common observation from the shear stress-displacement curves in Figures 14 to 18 is that at
608 higher applied displacement rates, the shear stresses during the initial displacements are high,
609 as indicated by the steep slope of the curve when the DST begins. This initial steepness suggests
610 that at higher displacement rates, shear forces in the samples are rapidly mobilized as the
611 particles are forced to respond quickly to the applied horizontal shearing. However, as the
612 displacement rate decreases, the initial portion of the curve shifts to a more gradual slope. This
613 is because slower displacement rates allow the soil particles more time to adjust, interlock, and
614 distribute the applied load more evenly, leading to a more progressive buildup of shear stress.
615 As shearing continues, the shear stress increases steadily for lower displacement rates,

ultimately yielding significantly higher peak stresses at failure compared to those at higher displacement rates. This is because slower displacement rates give particles additional time to rearrange and establish stronger interparticle contacts, enhancing frictional resistance and apparent cohesion. Consequently, lower displacement rates allow the soil to mobilize its full shear strength, while higher rates lead to a quicker but less complete mobilization.

4. Conclusion

This study investigates the shear behavior of two homogeneous samples RS and BS, and reconstituted varved clay couplets under varying normal stresses, moisture conditions, and displacement rates using the DST. The key findings are summarized as follows:

1. For all samples subjected to DST, the peak shear stress at failure increases with applied normal stresses, whereas the shear strength parameters and peak shear stress for all three sample types increase as the displacement rate at which the sample is sheared decreases. This trend is consistent across all moisture conditions.
2. However, the impact of variable factors differs among the three soil types. Both shear strength parameters—cohesion and internal friction angle—in the homogeneous RS samples exhibit the highest sensitivity to varying moisture conditions, which is evident from steep curve transitions between water contents. In general, the reconstituted couplet shows the least sensitivity in cohesion and friction angle for samples compacted at water contents around the OMC and beyond. These observations hold true across all displacement rates of 1.25 mm/min, 0.24 mm/min, and 0.024 mm/min.
3. The displacement rate significantly influences shear strength mobilization in all soil samples under a given normal stress. At a higher displacement rate of 1.25 mm/min, the shear stress-displacement curves show a steeper initial slope; however, samples sheared at this rate display the lowest peak stresses due to limited time for interparticle adjustment. As the displacement rate decreases, the initial shear stress slope becomes more gradual, where peak shear stress magnitudes increase as displacement rates decrease.
4. Peak shear stresses at failure, cohesion, and friction angle vary with changing moisture conditions. These variables increase with added moisture, achieving peak values between 0.8 OMC and OMC. After reaching these peak values, the parameters decrease as moisture continues to increase. The lowest values for peak shear stresses, cohesion, and friction angle are observed when the DST is conducted in dry soil conditions.

5. The change in displacement rate across soil samples results in significantly greater variation in cohesion than in the friction angle, which indicates that cohesion is more sensitive to changes in displacement rates compared to the angle of internal friction.
6. For homogeneous RS and BS samples, peak shear stress at failure in DST generally occurs when samples are compacted to a moisture content around OMC at displacement rates of 1.25 mm/min and 0.024 mm/min. For reconstituted varved clay couplets, however, peak stresses are observed in samples compacted at a slightly lower moisture content of approximately 0.8 OMC under the same shearing rates in DST. When tested at an intermediate displacement rate of 0.24 mm/min, homogeneous RS samples reach peak shear stress at 0.8 OMC, whereas homogeneous BS and couplet samples achieve peak shear stress at moisture content corresponding to OMC in DST.

In summary, this study emphasizes the importance of understanding the interactions among moisture content, displacement rate, and soil composition in determining shear strength behavior. The findings suggest that soils of varying compositions respond differently to moisture and loading conditions, which impacts their performance in engineering applications. Insights from this research can guide more effective geotechnical design practices in glacial environments where soils experience variable moisture and loading conditions due to glacial retreat, advancement, and movement. Future studies could further investigate the role of cyclic loading and long-term moisture changes to deepen the understanding of shear behavior in complex soil structures in glaciatic regions.

5. Acknowledgement

This study belongs to a part of the project 'Study of Glacial Dynamics and Sustainable Hydrological Resources in Arunachal Himalaya' (Project No. DST/CCP/MRDP/185/2019(G) dated 13/03/2020). The project is supported by Department of Science & Technology (SPLICE – Climate Change Program), Ministry of Science and Technology, Govt. of India. The authors express their gratitude for receiving the financial support for the same.

References

- Abdullahi, I., Imoh, U.U., Apata, A.C. (2022). Effect of Varying Moisture Content on Shear Strength Properties of Soil. Saudi Journal of Civil Engineering, 6(11): 256-263. http://doi.org/10.36348/sjce.2022.v06i11.001

- Altuhafi, F.N, Baudet, B.A., Sammonds, P. (2009). On the time-dependent behaviour of glacial sediments: a geotechnical approach. Quaternary Science Reviews, 28 (7-8): 693-707. https://doi.org/10.1016/j.quascirev.2008.07.016\
- Altuhafi, F.N, Baudet, B.A., Sammonds, P. (2010). The mechanics of subglacial sediment: An example of new "transitional" behaviour. Canadian Geotechnical Journal, 47(7): 775-790. https://doi.org/10.1139/T09-136
- ASTM. 2011. Standard test method for direct shear test of soils under consolidated drained conditions. ASTM D3080/D3080M. West Conshohocken, PA: ASTM.
- Basudhar, P.K., Acharya, I.P., Anubhav (2020). Strain Rate Effect on Shear Strength of Rounded and Angular Sand. In: Latha Gali, M., P., R.R. (eds) Geotechnical Characterization and Modelling. Lecture Notes in Civil Engineering, vol 85. Springer, Singapore. https://doi.org/10.1007/978-981-15-6086-6_15
- Beren, M., Çobanoglu, I., Çelik, S., Undul, O. (2020). Shear Rate Effect on Strength Characteristics of Sandy Soils. Soil Mechanics and Foundation Engineering, 57(4): 281–287. https://doi.org/10.1007/s11204-020-09667-y
- Bláhová, K., Ševelová, L., Pilařová, P. (2013). Influence of water content on the shear strength parameters of clayey soil in relation to the stability analysis of a hillside in Brno region. Acta Universitatis Agriculturae et Silviculturae Mendelianae Brunensis, 2013, LXI, No. 6, pp. 1583–1588. http://dx.doi.org/10.11118/actaun201361061583
- Blondeau, K. M. (1975). Sedimentation and stratigraphy of the Mount Rogers Formation, Virginia. Louisiana State University and Agricultural and Mechanical College, Geology and Geophysics. LSU Historical Dissertations and Thesis. https://doi.org/10.31390/gradschool_disstheses.8236
- Boulton, G.S., Dobbie, K.E. (1998). Slow flow of granular aggregates: the deformation of sediments beneath glaciers. Proceedings of the Royal Society A: Mathematical, Physical and Engineering Sciences, 356(1747). https://doi.org/10.1098/rsta.1998.0294
- Boulton, G.S., Dobbie, K.E., Zatsepin, S. (2001). Sediment deformation beneath glaciers and its coupling to the subglacial hydraulic system. Quaternary International, 86(1): 3-28. https://doi.org/10.1016/S1040-6182(01)00048-9
- Bureau of Indian Standards. (1980). IS:2720 (Part 3/Sec-2)-1980 (Methods of test for soils: Determination of specific gravity - Part 3/Section 2: Fine, medium, and coarse-grained soils). Bureau of Indian Standards, New Delhi, India.

- Bureau of Indian Standards. (1980). IS:2720 (Part 4)-1980 (Methods of test for soils: Grain size analysis). Bureau of Indian Standards, New Delhi, India.
- Bureau of Indian Standards. (1983). IS:2720 (Part 7)-1983 (Methods of test for soils: Determination of water content-dry density relation using light compaction). Bureau of Indian Standards, New Delhi, India.
- Bureau of Indian Standards. (1985). IS:2720 (Part 5)-1985 (Methods of test for soils: Determination of liquid limit and plastic limit). Bureau of Indian Standards, New Delhi, India.
- Chung, C.K., Finno, R.J. (1992). Influence of depositional processes on the geotechnical parameters of Chicago glacial clays. Engineering Geology, 32: 225-242. https://doi.org/10.1016/0013-7952(92)90050-9
- Cokca, E., Erol, O., Armangil, F. (2004). Effects of compaction moisture content on the shear strength of an unsaturated clay. Geotechnical and Geological Engineering, 22: 285–297. https://doi.org/10.1023/B:GEGE.0000018349.40866.3e
- Dobak, P., Kiełbasiński, K., Szczepański, T., Zawrzykraj, P. (2018). Verification of compressibility and consolidation parameters of varved clays from Radzymin (Central Poland) based on direct observations of settlements of road embankment. Open Geosciences, 10(1): 911-924. https://doi.org/10.1515/geo-2018-0072
- Du, H., Ma, W., Zhang, S., Zhou, Z., Liu, E. (2016). Strength properties of ice-rich frozen silty sands under uniaxial compression for a wide range of strain rates and moisture contents. Cold Regions Science and Technology, 123: 107-113. https://doi.org/10.1016/j.coldregions.2015.11.017
- Eden, W.J. (1955). A laboratory study of varved clay from Steep Rock Lake, Ontario. National Research Council Canada. Report (National Research Council of Canada. Division of Building Research), no. DBR-R-24 (1 December 1954). https://doi.org/10.4224/20331506
- Ehlers, J. (2022). From Moulins to Glacial Valleys. In: The Ice Age. Springer, Berlin, Heidelberg. https://doi.org/10.1007/978-3-662-64590-1_5
- Eigenbrod, K.D., Burak, J.B. (1991). Effective stress paths and pore-pressure responses during undrained shear along the bedding planes of varved Fort William Clay. Canadian Geotechnical Journal, 28 (6): 804-811. https://doi.org/10.1139/t91-097

- Eyles, N., Lazorek, M. (2013). Glacial Landforms, sediments |Glaciogenic Lithofacies. Encyclopedia of Quaternary Science, (2): 18-29. https://doi.org/10.1016/b978-0-444-53643-3.00084-4.
- Flieger-Szymanska, M., Machowiak, K., Krawczyk, D., Wanatowski, D. (2019) Characterisation of mineral composition and strength parameters of varved clays. In: Proceedings of the 17th European Conference on Soil Mechanics and Geotechnical Engineering (ECSMGE 2019). XVII ECSMGE 2019, 01-06 Sep 2019, Reykjavik, Iceland. International Society for Soil Mechanics and Geotechnical Engineering. https://doi.org/10.32075/17ECSMGE-2019-0172
- Florkiewicz, A., Flieger-Szymanska, M., Machowiak, K., Wanatowski, D. (2014). Engineering properties of varved clays from the Junikowski Stream Valley in Poland. In Conference: proceedings 4th International Conference on Geotechnical Engineering for Disaster Mitigation and Rehabilitation (4th GEDMAR) At: Kyoto, Japan, Volume: Geotechnics for Catastrophic Flooding Events.
- Hang, T. (2003). A local clay-varve chronology and proglacial sedimentary environment in glacial Lake Peipsi, Eastern Estonia. Boreas, 32(2): 416-426. https://doi.org/10.1111/j.1502-3885.2003.tb01094.x
- Horn, R., Albrechts, C. (2002). Stress strain effects in structured unsaturated soils on coupled mechanical and hydraulic processes. 2002 ASAE Annual Meeting. http://doi.org/10.13031/2013.10376
- Huo, D., Bishop, M.P., Bush, A.B.G. (2021). Understanding Complex Debris-Covered Glaciers: Concepts, Issues, and Research Directions. Frontiers in Earth Science, (9). https://doi.org/10.3389/feart.2021.652279
- Kang, Q., Xia, Y., Li, X., Zhang, W., Feng, C. (2022). Study on the Effect of Moisture Content and Dry Density on Shear Strength of Silty Clay Based on Direct Shear Test. Advances in Civil Engineering, 22(1): 2213363. https://doi.org/10.1155/2022/2213363
- Kazi, A. (1968). Aspects of the Engineering Geology of Laminated Glacial Lake Clays. Thesis, Imperial College of Science London.
- Krawczyk, D., Flieger-Szymańska, M. (2018). The value of plasticity index (IP) and liquidity index (IL) of North Polish ablation boulder clays and varved clays depending of the method of its determination. Scientific Review Engineering and Environmental Sciences (SREES) 27(2), 167-174. http://doi.org/10.22630/PNIKS.2018.27.2.16

- Lacasse, S.M., Ladd, C.C., Barsvary, A.K. (1977). Undrained behavior of embankments on New Liskeard varved clay. Canadian Geotechnical Journal, 14(3): 367-388. https://doi.org/10.1139/t77-041
- Lamoureux, S.F., Bradley, R.S. (1996). A late Holocene varved sediment record of environmental change from northern Ellesmere Island, Canada. Journal of Paleolimnology, 16: 239–255. https://doi.org/10.1007/BF00176939
- Leroueil, S., Bouclin, G., Tavenas, F., Bergeron, L., Rochelle, P.L. (1990). Permeability anisotropy of natural clays as a function of strain. Canadian Geotechnical Journal, 27(5): 568-579. https://doi.org/10.1139/t90-072
- Lindqvist, J. K., Lee, D.E. (2009). High-frequency paleoclimate signals from Foulden Maar, Waipiata Volcanic Field, southern New Zealand: An Early Miocene varved lacustrine diatomite deposit. Sedimentary Geology, 222 (1–2): 98-110. https://doi.org/10.1016/j.sedgeo.2009.07.009
- Lydzba D., Tankiewicz M. (2012). Preliminary study of failure anisotropy characterization of varved clay. AGH Journal of Mining and Geoengineering, 36 (2): 229-234.
- Mamo, B., Banoth, K.K., Dey, A. (2015). Effect of strain rate on shear strength parameter of sand. 50th Indian Geotechnical Conference, held between 17th -19th December 2015, Venue: College of Engineering, Pune, Maharashtra, India.
- Mark, B.G., Fernández, A. (2022). The Glacial Waterscape: Glaciers and Their Unique Geomorphological Connection to Society. Treatise on Geomorphology, 2(4): 281-289. https://doi.org/10.1016/B978-0-12-818234-5.00125-5
- Menzies, J. van der Meer, J.J.M. (2018). Chapter 1 – Introduction. Past Glacial Environments (Second Edition), pp. 1-13. https://doi.org/10.1016/B978-0-08-100524-8.00027-0
- Paterson, W.S.B. (1994). The Physics of Glaciers. (third ed.), Elsevier, NY (1994).
- Philippe, E.G.H., St-Onge G., Valet J.P., Godbout P.M., Egli R., Francus P., Roy M. (2023). Influence of seasonal post-depositional processes on the remanent magnetization in varved sediments from glacial lake Ojibway (Canada). Geochemistry, Geophysics, Geosystems, 24(3). https://doi.org/10.1029/2022GC010707
- Rasti, A., Adarmanabadi, H.R., Pineda, M., Reinikainen, J. (2021). Evaluating the Effect of Soil Particle Characterization on Internal Friction Angle. American Journal of

Engineering and Applied Sciences, 14(1): 129-138. http://doi.org/10.3844/ajeassp.2021.129.138

- Ringberg, B., Erlström, M. (1999). Micromorphology and petrography of Late Weichselian glaciolacustrine varves in southeastern Sweden. CATENA, 35 (2–4), 147-177. https://doi.org/10.1016/S0341-8162(98)00098-8
- Schneider, M.A., Whittle, R.W., Springman, S.M. (2022). Measuring strength and consolidation properties in lacustrine clay using piezocone and self-boring pressuremeter tests. Canadian Geotechnical Journal, 59(12): 2135-2150. https://doi.org/10.1139/cgj-2021-0486
- Tankiewicz, M. (2015). Experimental Investigation of Strength Anisotropy of Varved Clay. Procedia Earth and Planetary Science, 15: 732-737. https://doi.org/10.1016/j.proeps.2015.08.116
- Tankiewicz, M. (2016). Structure investigations of layered soil – varved clay. Annals of Warsaw University of Life Sciences - SGGW Land Reclamation, 48(4), 365-375. http://doi.org/10.1515/sggw-2016-0028
- Thermann, K., Gau, C., Tiedemann, J. (2006). Shear strength parameters from direct shear tests - influencing factors and their significance. The Geological Society of London, IAEG 2005, Paper number 484.
- Tornborg, J., Karlsson, M. and Karstunen, M. (2023). Permanent sheet pile wall in soft sensitive clay. Journal of Geotechnical and Geoenvironmental Engineering, 149(6). https://doi.org/10.1061/JGGEFK.GTENG-10955
- Zhang, Y., Lu, J., Han, W., Xiong, Y., Qian, J. (2023). Effects of Moisture and Stone Content on the Shear Strength Characteristics of Soil-Rock Mixture. Materials, 16(2), 567. https://doi.org/10.3390/ma16020567
- Zhou, G.G.D., Leilei, C., K.F.E., Song, D., Mu, Q. (2019). Effects of Water Content on the Shear Behavior and Critical State of Glacial Till in Tianmo Gully of Tibet, China. Journal of Mountain Science, 18(8):1743-1759. http://doi.org/10.1007/s11629-019-5440-9